Bulletin of the Seismological Society of America, Vol. 92, No. 7, pp. 2761–2781, October 2002

Paleoseismic Event Dating and the Conditional Probability of Large Earthquakes on the Southern San Andreas Fault, California

by Glenn P. Biasi, Ray J. Weldon II, Thomas E. Fumal, and Gordon G. Seitz

Abstract We introduce a quantitative approach to paleoearthquake dating and apply it to paleoseismic data from the Wrightwood and Pallett Creek sites on the southern San Andreas fault. We illustrate how stratigraphic ordering, sedimentological, and historical data can be used quantitatively in the process of estimating earthquake ages. Calibrated radiocarbon age distributions are used directly from layer dating through recurrence intervals and recurrence probability estimation. The method does not eliminate subjective judgements in event dating, but it does provide a means of systematically and objectively approaching the dating process. Date distributions for the most recent 14 events at Wrightwood are based on sample and contextual evidence in Fumal *et al.* (2002) and site context and slip history in Weldon *et al.* (2002). Pallett Creek event and dating descriptions are from published sources. For the five most recent events at Wrightwood, our results are consistent with previously published estimates, with generally comparable or narrower uncertainties. For Pallett Creek, our earthquake date estimates generally overlap with previous results but typically have broader uncertainties. Some event date estimates are very sensitive to details of data interpretation. The historical earthquake in 1857 ruptured the ground at both sites but is not constrained by radiocarbon data. Radiocarbon ages, peat accumulation rates, and historical constraints at Pallett Creek for event X yield a date estimate in the earliest 1800s and preclude a date in the late 1600s. This event is almost certainly the historical 1812 earthquake, as previously concluded by Sieh *et al.* (1989). This earthquake also produced ground deformation at Wrightwood.

All events at Pallett Creek, except for event T, about A.D. 1360, and possibly event I, about A.D. 960, have corresponding events at Wrightwood with some overlap in age ranges. Event T falls during a period of low sedimentation at Wrightwood when conditions were not favorable for recording earthquake evidence. Previously proposed correlations of Pallett Creek X with Wrightwood W3 in the 1690s and Pallett Creek event V with W5 around 1480 (Fumal *et al.*, 1993) appear unlikely after our dating reevaluation. Apparent internal inconsistencies among event, layer, and dating relationships around events R and V identify them as candidates for further investigation at the site. Conditional probabilities of earthquake recurrence were estimated using Poisson, lognormal, and empirical models. The presence of 12 or 13 events at Wrightwood during the same interval that 10 events are reported at Pallett Creek is reflected in mean recurrence intervals of 105 and 135 years, respectively. Average Poisson model 30-year conditional probabilities are about 20% at Pallett Creek and 25% at Wrightwood. The lognormal model conditional probabilities are somewhat higher, about 25% for Pallett Creek and 34% for Wrightwood. Lognormal variance $\sigma_{\ln}$ estimates of 0.76 and 0.70, respectively, imply only weak time predictability. Conditional probabilities of 29% and 46%, respectively, were estimated for an empirical distribution derived from the data alone. Conditional probability uncertainties are dominated by the brevity of the event series; dating uncertainty contributes only secondarily. Wrightwood and Pallett Creek event chronologies both suggest variations in recurrence interval with time, hinting that some form of recurrence rate modulation may be at work, but formal testing shows that neither series is more ordered than might be produced by a Poisson process.

Introduction

Paleoseismic researchers integrate a number of sources of information to estimate paleoearthquake dates. Absolute dating constraints derive from radiocarbon, thermoluminescence, or similar methods. Trench mapping provides relationships among stratigraphic and structural features and absolute dates. Observations of soil development and organic sediment accumulations provide indications of time passage. The complexity of this evidence has led some workers to simplify the available information or to use only parts of it quantitatively. For example, dendrochronologically calibrated radiocarbon date distributions may be reduced to a mean and standard deviation or even to an age range with an implicit uniform distribution. As this simplification involves subjective choices, it becomes difficult to evaluate the impact of those choices on the final results. Also, when different workers make different choices it becomes difficult to compare their results. The method presented here attempts to provide a framework within which to integrate the available objective data and to provide a basis of agreement from which to consider more subjective or interpretative steps. The framework can be applied to layer dates, earthquake date estimates, recurrence intervals, and as a means to evaluate overall data consistency. The proposed approach also allows the interpreter to see which constraints are most important and where additional field measurements or dating constraints would be most valuable.

We illustrate the approach with multiple event records from Wrightwood (Fumal *et al.*, 1993, 2002) and Pallett Creek (Sieh, 1984; Sieh *et al.*, 1989), 26 km apart on the southern San Andreas fault (Fig. 1). In studies of the San Andreas fault, paleoseismology has been essential in assessing its seismic potential because the instrumental and historical records are too short to adequately characterize earthquake recurrence. Models of fault segmentation and event correlation developed from paleoseismic studies here are applied worldwide.

Layer Dating

Paleoearthquake dating begins by obtaining stratigraphic information of layer ordering, thicknesses, and crosscutting relationships and combining them with ^{14}C ages from these layers. The layer date estimation aspect of this problem was previously presented by Biasi and Weldon (1994). We briefly review that methodology because their results are used as a starting point for earthquake dating in this article.

Radiocarbon ages can be associated by a calibration process (Stuiver and Reimer, 1993) with a probability distribution function (pdf) describing how likely it is that the sample formed in any given calendar interval. The calibrated distributions are often multimodal (e.g., Fig. 2) and usually not well characterized by a mean and standard deviation. For convenience we have called dated horizons "layers," and their date distributions are symbolized as $p_{Li}(x)$ for layers $i = 1, \ldots, n$. Layer date distributions can be broad because they incorporate sample ^{14}C age uncertainties, the laboratory multiplier, and the uncertainty in the calibration curve. If the true formation order among layers is known from stratigraphic relationships, this information can often reduce the range of likely dates during which individual layers formed. If, in addition, some minimum amount of time is known to separate layers, their age ranges can be further narrowed. Mathematically the refinement process can be stated as a conditional probability problem, where the unconditional probability comes from the original date distribution and the

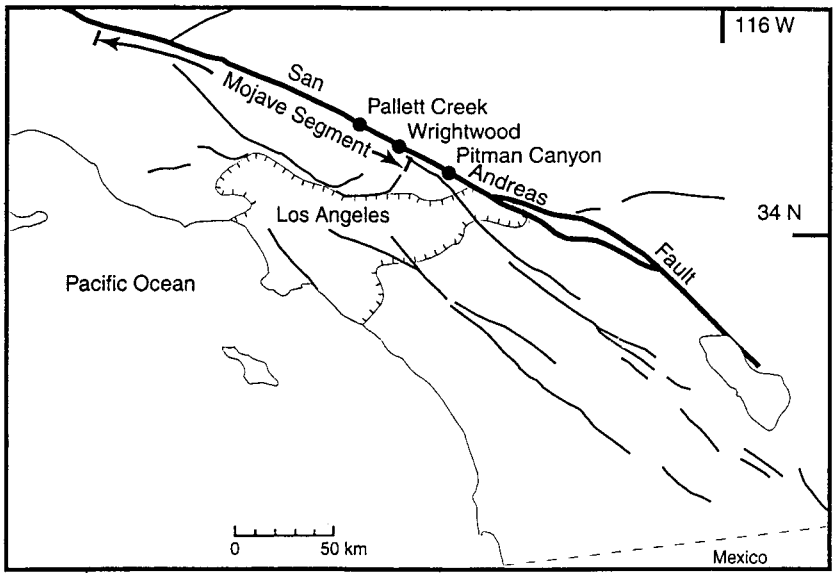

Figure 1. Location of the Wrightwood, Pallett Creek, and Pitman Canyon sites in southern California. The heavy line is the San Andreas fault; lighter lines are secondary faults in the region. The Mojave segment has been variously defined but is shown here as the straight segment between the Big Bend and the southern extent of the 1857 rupture (Sieh, 1978b). Metropolitan Los Angeles (hatchured) could experience strong ground motions if the Mojave segment ruptured alone or as part of a larger event.

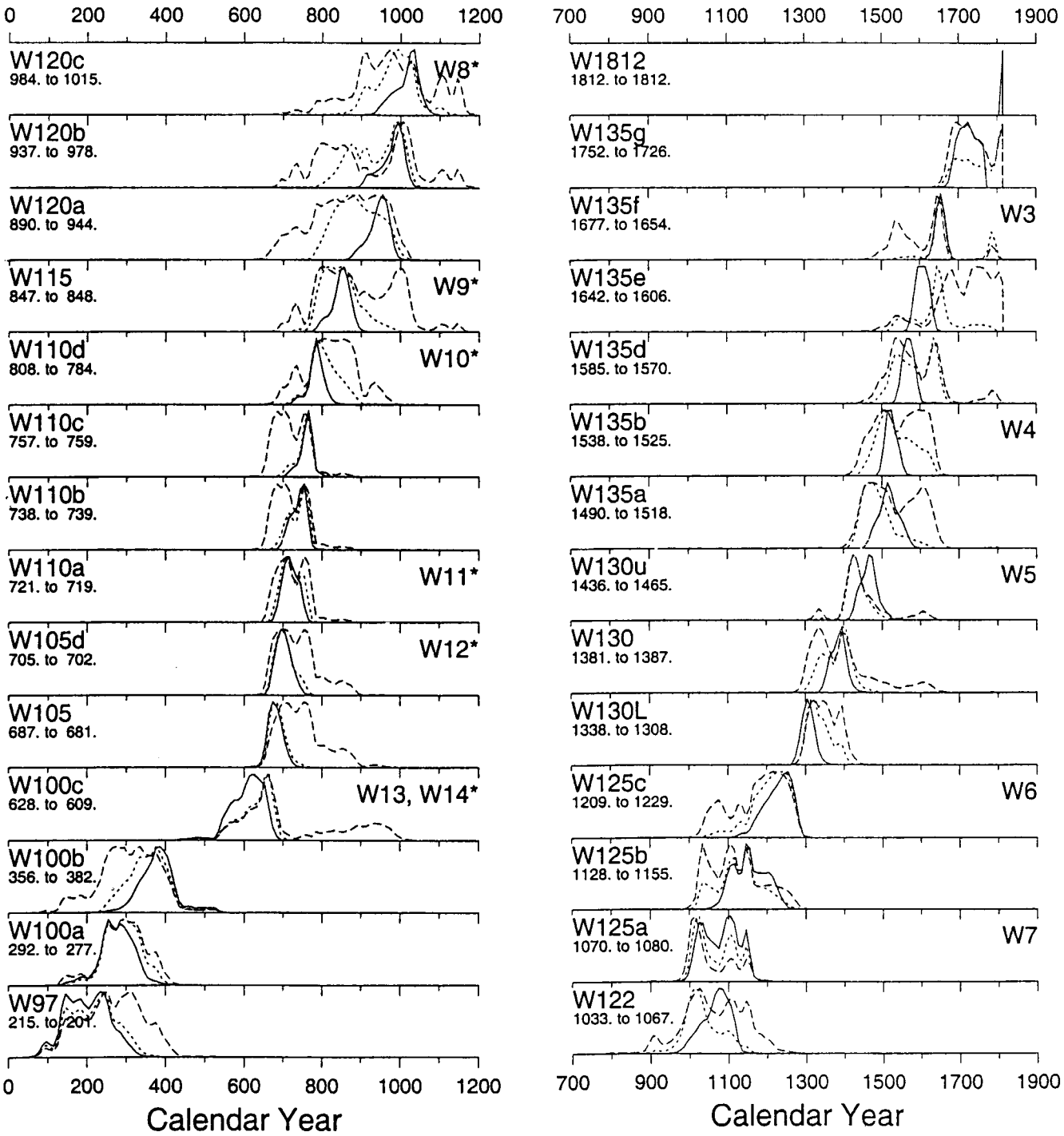

Figure 2. Calibrated layer dates (dashed), ordering-constrained distributions (dotted), and sedimentation-plus-ordering-constrained (solid) distributions for Wrightwood layers. Under the layer names on the left side are mean dates for the ordering only and the sedimentation-plus-ordering (fully) constrained distributions, respectively. The term "layer" refers to a stratigraphic unit from which one or more radiocarbon (RC, or ^{14}C) ages has been determined. Layer assignments and sample ^{14}C ages are given in Appendix 1. Sample descriptions and site context are given in Fumal *et al.* (1993, 2002) and Weldon *et al.* (2002). Vertical scaling differs within each layer plot to give each distribution the same peak height. The stratigraphic positions of ground ruptures at Wrightwood (W3, W4, . . .) are shown on the right-hand side. Event names with stars occurred during the layer formation.

condition is stratigraphic ordering or ordering with some time separation between layers (Biasi and Weldon, 1994). For Wrightwood and Pallett Creek, ordering and time separations inferred from peat thicknesses and accumulation rates were used to constrain layer dates. Other geologic constraints could be considered, such as soil development, varved lake sediments, bioturbation, or erosion. The particular choices of constraints are up to the interpreting paleoseismologist, but the methodology provides a way to use them as objectively and uniformly as possible.

The layer age results for Wrightwood and Pallett Creek are shown in Figures 2 and 3. Wrightwood results (Fig. 2) are based on layer and event chronologies discussed in Fumal *et al.* (2002) and Weldon *et al.* (2002). Appendix 1 gives the radiocarbon age and layer association of individual samples. Calibrated date distributions for multiply sampled layers were derived by summing the individual calibrated distributions and dividing by the number summed. This gives each sample equal weight as an estimate of when the layer was formed. This approach was preferred to one of combining radiocarbon ages before calibration because relatively few samples could be considered true replicates. Some samples were not used because of documented biases caused by the sample pretreatment method. Seitz (1999) and Fumal *et al.* (2002) discuss the cause of the bias in detail. Pallett Creek sample layer results (Fig. 3) follow Biasi and Weldon (1994) with two modifications. First, a date in layer P52 was shown in Biasi and Weldon (1994) as inconsistent with many adjoining layers and is removed here. Second, for reasons discussed in subsequent sections, P72 was also inconsistent and not used in ordering or full constraint cases.

Ordering alone reduces the variance of layer dates by 54% and 63% for Wrightwood and Pallett Creek relative to the original calibrated date distributions. The sedimentation-plus-ordering constrained layer date distributions for Wrightwood and Pallett Creek (solid lines, Figs. 2 and 3) using peat accumulation rate estimates (Fig. 4) are narrower and better defined. The constrained distributions usually focus on a single mode of their prior distributions, but they are still not Gaussian. The sedimentation-plus-ordering (hereafter called "fully") constrained distributions comprise our most complete information about the dates of layer formation.

Ordering among layer dates may also be used to test for consistency among nearby layer date distributions. If a series of layers formed in calendric order, the age of an individual layer should be approximately predicted by the ages of neighboring layers. A layer date pdf can be predicted by replacing it with a uniform distribution at least as wide as the extremes of the layers chronologically before and after it. One then applies the ordering constraints from neighboring layers to predict the age distribution of the layer under consideration and compares the result to the original calibrated distribution. Strong overlap means that the date distribution is well predicted by its neighbors, and weak overlap implies that it is not. Applying this method to the present

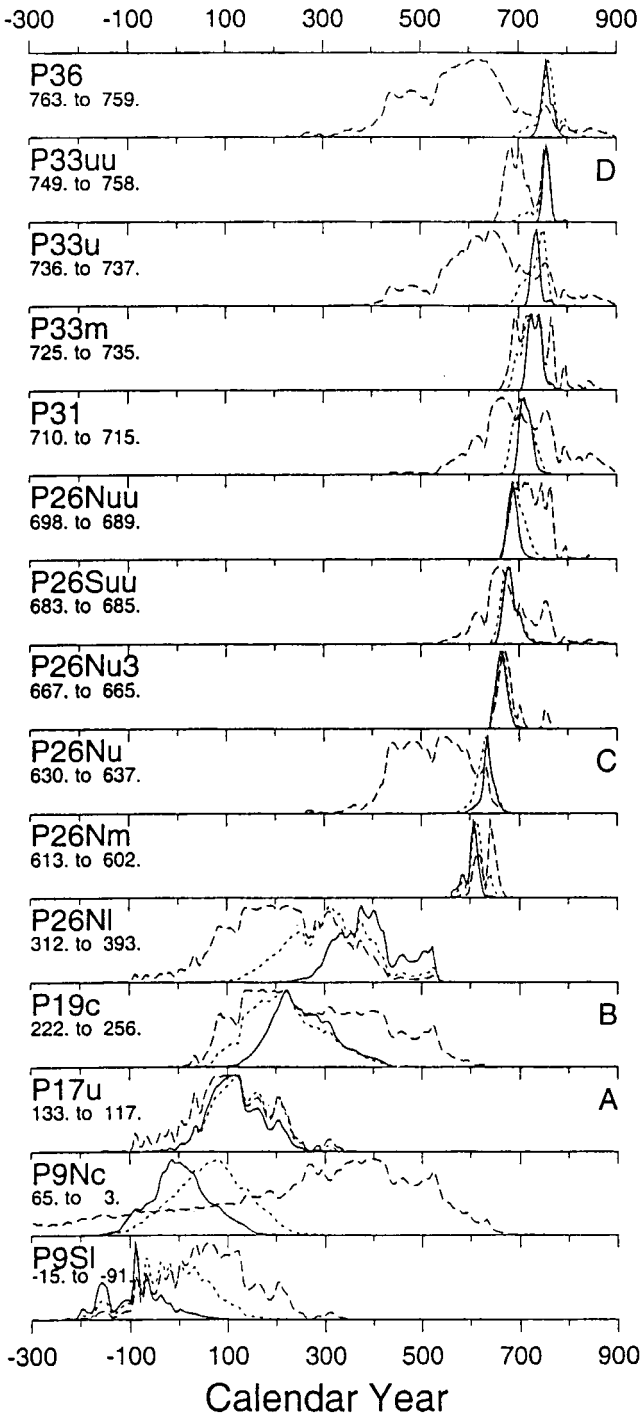

Figure 3. Caption on next page.

date series, we find that layer ages for P26Nm and P72 at Pallett Creek are poorly predicted by ages of adjoining samples (Table 1). Figure 3 shows that P26Nm is consistent but poorly predicted because of the large gap in age between this layer and the layer below it. P72, on the other hand, is essentially out of order with the five ordered samples immediately below it, despite its being derived from replicated

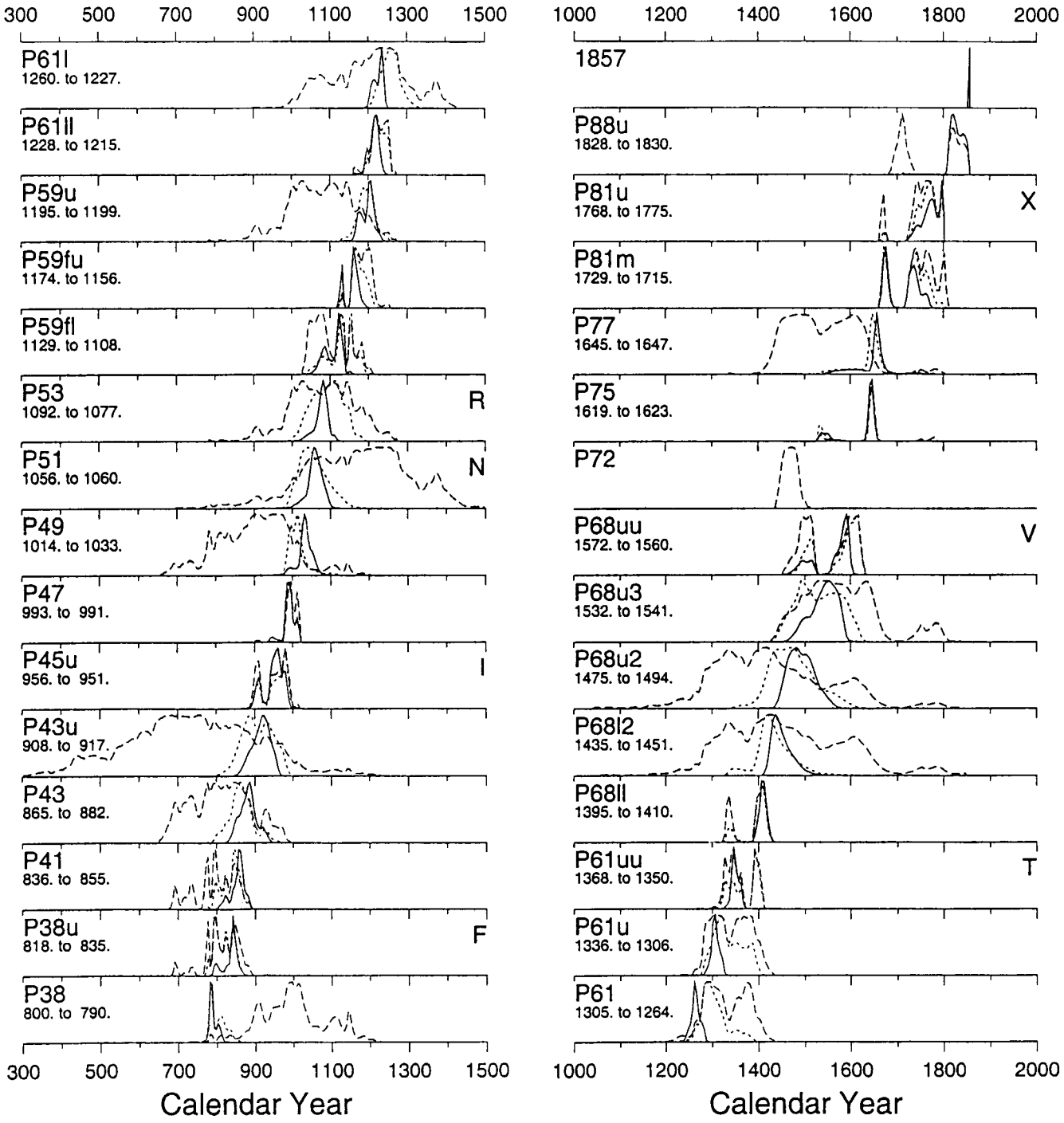

Figure 3. Calibrated layer dates (dashed), ordering-constrained distributions (dotted), and sedimentation-plus-ordering-constrained (solid) distributions for Pallett Creek. Plotting conventions are the same as for Figure 2. Seventy-five ^{14}C ages were available, some replicates of one another (Sieh, 1978a, 1984; Sieh *et al.*, 1989; K. Sieh, personal comm., 1992). Two of 75 ^{14}C ages and 4 of 47 layer date distributions were strongly inconsistent with surrounding data and were removed (Biasi and Weldon, 1994). The calibrated distribution for layer P72 is shown for reference but was not used to constrain layer dates. See text for details.

high-precision measurements. P72 overlies event V at Pallett Creek, so the implications of this result are discussed with that event. Similar out-of-sequence layers exist in the raw data at Wrightwood as well but were eliminated where contamination, usually by fine detrital charcoal, could be demonstrated (Seitz, 1999; Fumal *et al.*, 2002).

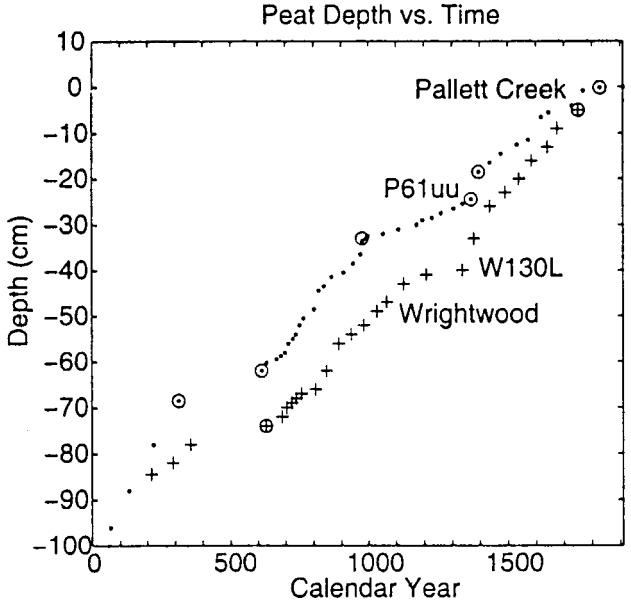

Figure 4. Peat accumulation plots for Pallett Creek and Wrightwood sites. Peat thicknesses were measured perpendicular to bedding at their thickest point. Measurements were compiled from mapped exposures and reported sample thicknesses. Thicknesses were plotted at the mean dates of their ordering constrained date distributions (dotted lines, Figs. 2, 3). Average peat accumulation rates were estimated where multiple dates define segments by drawing straight lines through the circles. Higher rates (smaller minimum time separation constraints) were used at "growth spurts" where the average rate would otherwise force nearby layer dates into unlikely posterior distributions. For Wrightwood a single rate of 15 yr/cm was applied because the available data do not justify a more detailed model. Pallett Creek peat accumulation resolvably varied with time. Both sites experienced slow accumulation from A.D. 350–600. Event W14 occurred during this slow period and is poorly resolved as a result.

Event Dating

In most cases an "event horizon" identified by the paleoseismologist is inferred to be the ground surface at the time of an earthquake that ruptured or folded sediments at the site. The association of geologic disruption with a significant earthquake is an inference and derives from the detailed site geologic investigations (Sieh *et al.*, 1989; Fumal *et al.*, 1993; Weldon *et al.*, 2002). To estimate the date of ground rupture we prefer to bound its age using the layer dates above and below the event horizon rather than identifying the event with either bounding layer date distribution. In most cases the amount of time between sample formation and the ground rupture itself is not known. On the other hand the stratigraphic order of layers and events is generally accepted to provide firm limits on the event date. To approach event bounding consistently we identify the layer date with the stratigraphic middle of the sample(s) from the layer, as was done in Sieh *et al.* (1989). For the samples considered here, sample centers are separated by a centimeter or more of peat, which, for the peat growth rates we estimate, is comparable to the resolution of high-precision age determinations that comprise much of the data. Even when a peat is buried by an earthquake-generated sand blow and then resumes accumulation (Sieh, 1984; Sieh *et al.*, 1989), some time is required to accumulate a thickness sufficient to sample. In peat-rich sections such as Wrightwood and Pallett Creek, event dating accuracy is ensured by bounding the event. Precision is often recovered as well because quantifiable constraints can be inferred from peat thicknesses and accumulation rates. Using all available constraints increases the degree of uniformity and objectivity in handling the data and tends to reduce the impact of an inconsistent sample taken near an event horizon.

Event date estimation is illustrated in Figure 5. We know that the event happened between the true dates of the two bounding layers. Given two perfect bounding dates (e.g., historical dates before and after an earthquake) (Fig. 5a) and no additional information, the event would be considered equally likely to have occurred at any time between the two dates. The event date distribution is then a uniform distribution between the dates. If the bounding dates have some uncertainty, but do not overlap (Fig. 5b), the event is still equally likely between them, as is reflected by the flat middle section of the event date distribution. However, with some probability, the event could have occurred within the range of the older bounding layer date, so long as the true layer date is older than the event and within its range. A symmetrical situation exists for the younger layer date. The event date distribution follows the cumulative and complimentary cumulative distributions of the bounding layers and is flat between their interior tails. Where the bounding dates overlap (Fig. 5c), the method is the same, even though there is no longer a flat region between them. The overlapping case introduces a mathematical complexity that the true values of the bounding layers depend on each other through ordering and are not strictly independent, but this problem is readily addressed.

Table 1
Consistency of Calibrated Date Distributions for Selected Layers at Pallett Creek with Those Predicted by the Age Distributions of Adjoining Layers

Layer	Percent of Prediction in Central 95% of Calibrated Layer Age
P26Nm	3
P26Nu	74
P36	100
P38	80
P68uu	50
P72	3

A value of about 50% for a bimodal distribution indicates that one or the other peak is preferred.

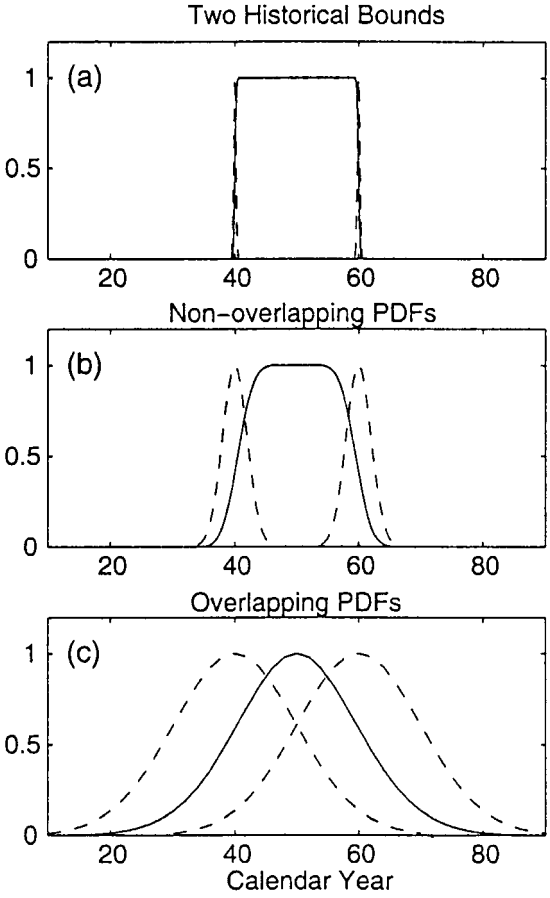

Figure 5. Conceptual approach for determining earthquake date distributions. Dating information modifies prior knowledge that the earthquake could have occurred at any time in the past. (a) Given two perfect dates and no other information, the earthquake is considered equally likely anywhere between them. (b) An analogous condition exists between the interior tails of uncertain dates—any time is equally likely. The earthquake also could have occurred within the distributions of either bounding date, but with lower probability, because the true layer date must be in the outer remainder of the distribution. (c) Overlapping layer dates are handled in an analogous manner, but for each possible earthquake date, both marginal distributions must be considered. As in (a), the event is still equally likely between any ordered pair of dates selected from the bounding layer dates.

If layer date distributions $p_{L_i}(x)$ and $p_{L_{i+1}}(x)$ bound event j, then the event dating method suggested by Figure 5 can be implemented by considering all possible pairs of dates $\{x_i, x_{i+1}\}$ and weighting by the probabilities that x_i and x_{i+1} are the true layer dates. The joint density function is given by

$$p(x_i,\ x_{i+1}) \ = \ C_1 p_{L_i}(x_i) p_{L_{i+1}}(x_{i+1}) \mathbf{1}, \qquad (1)$$

where $\mathbf{1}(\cdot) = 1$ for $x_i < x_{i+1}$, and 0 otherwise, and $C_1 = 1/$[sum of numerator] gives the resultant distribution unit area.

For any pair $\{x_i, x_{i+1}: x_i < x < x_{i+1}\}$ the uniform distribution between them is

$$p_{Ej}(x|x_i,\ x_{i+1}) \ = \ \frac{1}{x_{i+1} \ - \ x_i}. \qquad (2)$$

The constraint $x_i < x_{i+1}$ implements what the stratigraphy tells us, namely, that the earthquake might have occurred at any time between the true dates of the layers.

The true layer dates of L_i and L_{i+1} are not known, but for any given x we can include all possible pairs $\{x_i, x_{i+1}\}$ by summing the probability contributions of each pair. The event date distribution is the marginal distribution

$$p_{Ej}(x|x_i < x_{i+1}) = \sum_{x_i, x_{i+1}: x_i < x < x_{i+1}} \frac{C_2 p_{L_i}(x_i) p_{L_{i=1}}(x_{i+1})}{x_{i+1} \ - \ x_i}. \qquad (3)$$

Constant C_2 is calculated like C_1 to give p_{Ej} unit area.

Equation (3) is an implementation of Bayes theorem. That is, it begins with prior information about the earthquake date and modifies that information based on the layer date distributions around it. The assumption (prior distribution) $\frac{1}{(x_{i+1} - x_i)}$ in equation (3) means that (1) the event is between the true ages of the layers; and (2) equally likely anywhere in that interval. The first of these restates the meaning of the layer and event stratigraphic relations. Criticism of it would have to focus outside the mathematical model and on the paleoseismic interpretation of the microstratigraphy. The second element of the assumption is the least informative implementation of the first (i.e., between the bounding layers, any date is as likely as any other). An even less restrictive strategy would be to assume that the event was equally likely in some larger interval, without reference to x_i or x_{i+1}. For example, if the layer dates are accepted as bounding the event, then the oldest nonzero date in $p_{L_i}(x)$ and the youngest in $p_{L_{i+1}}(x)$ define the widest range over which any prior can have an effect.

An alternative explanation of equation (3) can be visualized from Figure 5a. Instead of perfect layer dates with unit area at each end, the spikes can be interpreted as having the probabilities a pair at a time of the discrete elements of $p_{L_i}(x)$ and $p_{L_{i+1}}(x)$, bounding the event. Then the uniform distribution between them has width $W = (x_{i+1} \ - \ x_i)$, height $1/W$ (equation 2), and probability $p_{L_i}(x_i) p_{L_{i+1}}(x_{i+1})$. As different pairs of end points are considered, the uniform distributions are summed as described in equation (3).

Figure 5 also suggests when a uniform prior distribution between layer dates might not be appropriate. If recurrence is random or near random in time, then the uniform approximation is appropriate. If, on the other hand, a well-defined time-predictable earthquake recurrence model is known for the fault, then one might consider modifying equation (2) Neither of the event series considered in this article (and no

others of which we are aware) constrain a recurrence model well enough to propose such a modification.

When some minimum amount of time can be inferred between a bounding sample and the event horizon, this separation can be included as an additional constraint. If Δx_{i+} and $\Delta x_{(i+1)-}$ represent intervals of time to the event horizon after the ith and before the $(i + 1)$st layers, Equation (3) can still be used by modifying the range of summation such that $(x_i + \Delta x_{i+}) < x < (x_{i+1} - \Delta x_{(i+1)-})$. Constant C_2 still normalizes p_{Ej} but is numerically different from the case without sediment separations. We advocate these constraints because it encourages the interpreter to formalize and quantify timing relationships around the event horizon. For example, if evidence of a hiatus like a paleosol or an erosional event leads the paleoseismologist to conclude that the event horizon is "much closer in time" to one or other bounding layer, some minimum amount of time for the hiatus may be used, rather than simply associating the event with one of the bounding layers. In Table 2 we list the sedimentation partitioning we applied at event horizons to calculate fully constrained event date distributions.

Figure 6 shows earthquake date distributions for the Wrightwood and Pallett Creek sites. The dashed lines show event date distributions using the ordering-only layer dates from Figures 2 and 3. The solid line plots include sedimentation constraints between layers and at the event horizon. The fully constrained distributions comprise a uniform application of the most complete information available about when these paleoseismic events occurred. Table 3 summarizes event dates and distribution widths for each degree of constraint.

We discuss each event below and compare our results with previously published estimates (Sieh 1984; Sieh *et al.*, 1989; Fumal *et al.*, 1993). Throughout the article, event names *Wn* refer to Wrightwood event *n* (Fumal *et al.*, 2002) and single letter names refer to Pallett Creek events of Sieh *et al.* (1989).

Table 2
Sediment Partitioning at Event Horizons and Resulting Inferred Time Constraints

Event	Layer below Event	Years	Layer above	Years
Wrightwood Event Horizon Constraints				
W14	W100b	60	W105	−45
W13	W100c	30	W105	−15
W12	W105	15	W110a	−15
W11	W110a	15	W110b	−15
W10	W110c	15	W115	−60
W9	W110d	60	W120a	−90
W8	W120b	45	W122	−45
W7	W125a	30	W125b	−30
W6	W125c	10	W130L	−10
W5	W130u	20	W135a	−35
W4	W135b	10	W135d	−35
W3	W135f	10	W135g	−35
Pallett Creek Event Horizon Constraints				
C	P26Nu	0	P26Nu3	−10
D	P33uu	5	P36	−15
F	P38u	5	P41	−5
I	P45u	5	P47	−20
N	P51	30	P53	−10
R	P53	20	P59fl	−30
T	P61uu	10	P68ll	−50
V	P68uu	5	P75	−45
X	P81u	5	P88u	0

Thicknesses are estimates based on stratigraphic descriptions from Sieh (1978a, 1984), Sieh *et al.* (1989), and Fumal *et al.* (1993, 2002). Peat accumulation rates are from Figure 4. All entries have been rounded to the nearest five years to reflect how they are actually used in event constraint.

Wrightwood

1812 and 1857: These events are regarded as historical (Sieh, 1978b; Jacoby *et al.*, 1988; Fumal *et al.*, 1993) but are not independently constrained by radiocarbon age determinations.

Event W3: Event W3 is only broadly resolved by ordering constraint alone. Sedimentation constraints on layer dates and at the event horizon lead to a better defined estimate of A.D. 1685 (1647–1717). The estimate of Fumal *et al.* (1993), A.D. 1700 (1680–1730), is similar in width but somewhat younger in its mean and limits.

Event W4: The date range of Fumal *et al.* (1993) for event W4 (A.D. 1500–1640) is consistent with the range of the order-constrained date distributions and nearly centered on our fully constrained estimate, A.D. 1536 (1508–1569). Sediment constraints at the event horizon make our estimated range narrower than theirs.

Event W5: This event is ill constrained by bounding layers W130u and W135a alone, but like event W4, it is better defined with ordering because of the strong overlap of layer dates W130L and W130 below and W135b through W135f above (Fig. 2). Layer sedimentation constraints and sediment partitioning at the event horizon lead to an estimate of A.D. 1487 (1448–1518). Fumal *et al.* (1993) considered this event to be a couple of decades younger than W130u for their estimate, A.D. 1470 (1450–1490).

Evidence for events W6 through W14 are documented by Fumal *et al.* (2002). Discussion here is limited to how dating evidence culminates in event pdfs.

Event W6: Peat W125c was at the ground surface when this event left a fissure cutting to the top of the layer that was filled by subsequent deposition. We bounded W6 by W130L above and W125c below (Fig. 2). Peat constraints around W6 are weak, consisting of accumulation time for half the 1-cm thicknesses of the bounding layers. Our estimate, 1263 (1191–1305) is relatively broad because the range of ages allowed by samples within layer W125c (Appendix 1).

Event W7: This event occurred during the lowermost W125 stringer, W125a and before W125b. Event W7 would have a range of about 250 years based on bounding dates alone. Our estimate, 1116 (1047–1181) is narrower because peat thicknesses between the bounding dates (2 cm on each side of the event horizon) were included.

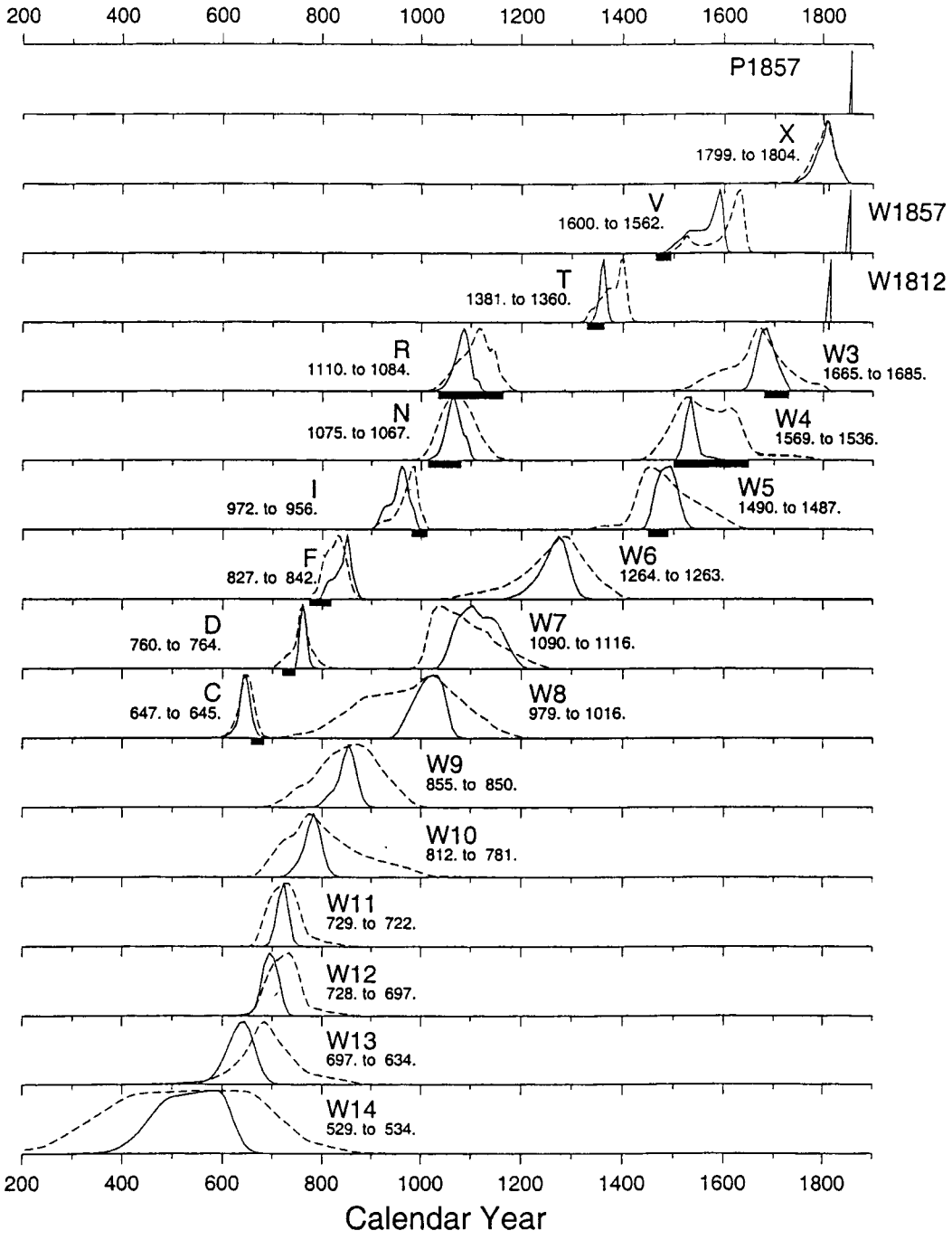

Figure 6. Wrightwood and Pallett Creek event date distributions. Dashed plots are events using ordering-constrained layer date distributions (dotted, in Figs. 2 and 3); solid lines show events from fully constrained layer distributions and peat thickness partitioning at the event horizon. Events W1812, W1857, and P1857 are shown as historic. Dates under the event names are the mean of the ordering-only and fully constrained event distributions, respectively. The heavy underbars indicate previously published two-sigma date ranges from Fumal *et al.* (1993) and Sieh *et al.* (1989). The vertical scale varies from event to event to give each distribution the same peak height.

Event W8: The stratigraphic location of event W8 within layer W120c cannot presently be resolved. Identifying event W8 with dates from this layer alone would allow event estimates from about 900 to 1160. Our estimate, 1016 (957–1056) spans under 40% of this range, profiting from ordering below to W110d and above to W125c.

Event W9: This event occurred within W115. Calibrated ages from this layer (Fig. 2) would only poorly con-

Table 3
Mean and 95% Range for Event Distributions Plotted in Figure 6*

	Fully Constrained		Ordering Only	
Event	Mean	95% Range	Mean	95% Range
Wrightwood				
W14	534	(407–628)	529	(329–676)
W13	634	(551–681)	697	(565–704)
W12	697	(657–722)	728	(664–743)
W11	722	(695–740)	729	(687–758)
W10	781	(736–811)	812	(731–894)
W9	850	(800–881)	855	(768–944)
W8	1016	(957–1056)	979	(864–1083)
W7	1116	(1047–1181)	1090	(1016–1194)
W6	1263	(1191–1305)	1264	(1158–1355)
W5	1487	(1448–1518)	1490	(1409–1546)
W4	1536	(1508–1569)	1569	(1482–1632)
W3	1685	(1647–1717)	1665	(1616–1796)
W1812	Historic			
W1857	Historic			
Pallett Creek				
C	645	(614–666)	647	(610–674)
D	764	(749–775)	760	(713–799)
F	842	(803–868)	827	(788–860)
I	956	(914–986)	972	(914–1003)
N	1067	(1031–1096)	1075	(1014–1137)
R	1084	(1046–1113)	1110	(1041–1165)
T	1360	(1343–1370)	1381	(1331–1410)
V	1562	(1496–1599)	1600	(1508–1641)
X	1804	(1758–1837†)	1799	(1746–1836†)

*Ranges of dates in this article include the center 95% of their respective date distributions.
†Allowing 1769–1837 within the historical period.

strain the event date. The timing of event W9 was estimated from W110d below and W120a above. A well-defined estimate of 850 (800–881) comes mainly from ordering constraint among neighboring layers and from correction for 6 cm of peat below W120a and 4 cm above W110d bounding event W9.

Event 10: Event W10 occurred sometime during the accumulation of layer W110d. The age of bounding layer W110c below is well constrained by ordering alone. Four centimeters of peat between W115 and event W10 constrain the event to a 75-year range around A.D. 781 (736–811).

Events W11 and W12: Event W11 around 722 (695–740) and W12, 697 (657–722) are largely constrained by ordering relationships in the range of W105–W110c. Peats in this part of the section occur in beds about 1 cm thick, with intervening clastics to improve temporal resolution. Event W11 illustrates a dating irony. Layers W110a, W110b, and W110c were sampled only once and thus appear better resolved than multiply sampled layers such as W115. In Figure 2 we give equal weight to each sample from layer W115 and recover similar resolution in the end because ordering among layers effectively selects most likely age ranges within each layer.

Events W13 and W14: Event W13 postdates layer W100c and the lowest stringer of peat W105. Unfortunately the carbon sample from W105a was strongly inconsistent with several samples from layers stratigraphically above it and seems to have been a root from several layers above. Event W14 occurred sometime during the formation of layer W100c. W13, with ordering of W105 through W110c above it yields a reasonably well defined estimate of 634 (551–681). A peat rate of 15 yr/cm is known to understate the time represented by these deep units, but finer resolution, especially of peat thickness, is not presently available. Event W14 is poorly constrained because layer W100c is massive, lacking intervening clastic deposits by which to divide the unit. Using layer W100b to constrain event W14 leads to a weakly constrained estimate of 534 (407–628). Layer W100c has a mean estimate of A.D. 609 (Fig. 2), so associating W14 with W100c would move the event estimate some 60 years later. However, Fumal *et al.* (2002) suggest that the age of W100c could be biased by the presence of roots from another layer. Event W14 illustrates the practical choice that can arise between an event date estimate from poor bounding dates and secure stratigraphy and an estimate from a single, better defined layer date that could be significantly in error. We note in passing that the small older tail of W100c and the younger tail of W100b are real and reflect a nearby "flat spot" in the calibration curve (Stuiver and Reimer, 1993). Layer date improvement by ordering among layers depends on overlap among ordered dates, so additional samples from this period would be especially valuable.

Pallett Creek

1857: This event is interpreted to be the historical January 1857 event by Sieh (1978b) and Sieh *et al.* (1989). The date of this event is consistent with, but not well constrained by, independent radiocarbon evidence.

Event X: The radiocarbon and stratigraphic data constrain event X to A.D. 1804 (1758–1837). All of the distribution is younger than A.D. 1745, and 94% lies after the start of the historical record in 1769 (Toppozada *et al.*, 1981). Major historical events are reported only in A.D. 1812 and 1857. Dendrochronological evidence (Jacoby *et al.*, 1988) indicates that the San Andreas fault 15 km southeast of Pallett Creek experienced a major earthquake between the fall of 1812 and the early spring of 1813. As previously concluded by Sieh *et al.* (1989), this evidence strongly implies that event X is the historic 8 December 1812 event. However, because Sieh *et al.* (1989) associated event X with samples from the event horizon (P81uu), they could not eliminate a small range of event X in the late 1600s. Fumal *et al.* (1993) cited this small range in event X to propose correlation with event We3, but our current analysis virtually rules out this possibility.

Event V: Our estimated date for event V 1562 (1496–1599) differs significantly from that of Sieh *et al.* (1989), 1480 (1465–1495), because of differences in handling the age of layer P72. The calendric ranges of P68uu and P72,

which bound event V, appear to tightly constrain event V but do so because the ^{14}C age of the overlying P72 is actually about 40 ^{14}C years older than the underlying P68uu (Table 4). Older radiocarbon ages can occur in younger layers at reversals in the calibration curve (e.g., Sieh *et al.*, 1989; from 1540 to 1610 in their Figure 2), but P72 radiocarbon ages cannot be explained by this possibility. Sieh *et al.* (1989) cited a small overlap of calendric ranges as the reason to treat the two high-precision measurements from P68uu and the three from P72 as replicates from a single layer, yielding a pooled ^{14}C age of 369 $\pm$ 6.7 years B.P. The pooled age focuses on a single-valued interval of the calibration curve and the small standard deviation of the ^{14}C age lead to a sharply defined event date.

A test for compatibility among ^{14}C samples (*T*-test, Ward and Wilson [1978], Case 1) indicates that the high precision ^{14}C ages bounding event V probably (94% rejection) are not replicates from a common radiocarbon age source. Note that all ^{14}C ages for layer P72 above the event horizon are older than any P68uu sample ages below it (Table 4). Also, if one uses their resulting standard deviation of 6.7 years, means for three of the five high-precision dates are three-standard deviations from the pooled mean (Table 4). In addition, about 15 mm of peat, which elsewhere in the section would represent 14 to perhaps 60 years, and aeolian unit 71 (Sieh, 1978a, Salyards *et al.*, 1992) separate the P68uu and P72 samples. These observations motivated a closer look at the data constraining event V.

The two samples from unit P68uu and the three from P72 were gathered as replicates from their respective layers, so we pooled radiocarbon ages for each layer separately and tested whether the true (not ^{14}C) ages might actually be equal (case II, Ward and Wilson, 1978). With 98% confidence one can say that the true ages of P68uu and P72 are different. The one-sided test P68uu $\geq$ P72 would be even more decisive. In other words, to be consistent, the true age of P68uu would have to be in the oldest few percent of its date distribution, and the true age of P72 would have to be in its youngest few percent. The probability of both, which is the condition for event V to be between them, is about two percent. Systematically younger age bias in layers below P72 seems unlikely since the younger carbon would have to come from above layer P72 without affecting P72 itself. From the statistical tests, the stratigraphic evidence, and as discussed earlier, the poor degree to which adjoining layer distributions would predict the P72 distribution (Table 1), we conclude that the measured age of layer P72 is too old for its stratigraphic position. K. Sieh (personal comm., 1993) did not consider sample contamination to be a likely explanation. However, Seitz (1999) and G. G. Seitz *et al.* (unpublished results), based on work at Pitman Canyon (Fig. 1) and reevaluation of Wrightwood dates, show that the presence of an older reworked carbon fraction can lead to a systematic bias toward older radiocarbon ages. Common laboratory pretreatment methods are not always effective at concentrating the carbon fraction that formed *in situ*. The pretreatment method used for the Pallett Creek high-precision dates (Sieh *et al.*, 1989) was acid only, which generally yields acceptable results; however, it would not have eliminated an older detrital charcoal fraction. Resampling and testing layers around event V will be needed to test this possible explanation.

Table 4
Radiocarbon Ages of Samples from Pallett Creek Layers P68uu and P72

Layer	Sample	C14 Age $\pm$ 1 std dev
P72	QL-1958	394.7 $\pm$ 12.2*
P72	QL-1994	374.0 $\pm$ 15.2*
P72	QL-1993	370.0 $\pm$ 15.4*
P72	USGS-136	437 $\pm$ 111
P68uu	QL-1956	344.5 $\pm$ 16.6*
P68uu	QL-1957	342.0 $\pm$ 16.5*
P68uu	USGS-137	289 $\pm$ 111

*High Precision

As an upper-bounding constraint, we used P75 minus the combined peat-derived constraints of P72 and below P75. Our date estimate of 1562 (1496–1599) is 82 years younger than that in Sieh *et al.* (1989) but corresponds reasonably well with that of Sieh (1984), who considered event V to be slightly younger than layer P68. The relatively broad date range for event V reflects the width of P68uu (Fig. 3), and the method of bounding events rather than associating it with either mode of the underlying layer.

Event T: This event is reasonably well constrained by the event-bounding layers P61uu and P68ll and well defined by sedimentation constraints. Although our uncertainty includes the date range of Sieh *et al.* (1989), our best estimate for event T (A.D. 1360, 1343–1370) is somewhat younger, at least in part because we added time above event T and beneath layer P68ll only for the peat deposited in the interval and not for the "extensive bioturbation" (Sieh *et al.* (1989), p. 611) or intervening clastic unit 65. We did not use bioturbation as a constraint because the amount of time represented by it and unit 65 are unknown and could be brief. If a minimum time period for bioturbation could be quantified, it could easily be added to the analysis. We did not add time for unit 65 because it might represent as little as a single storm event.

Event R: Data constraining event R come principally from sampling and descriptions in Sieh *et al.* (1989). They located event R beneath 20 cm of peat in unit 59 interpreted to have accumulated after the earthquake in a fissure opened by the event. The fragileness of the fissure indicated to Sieh *et al.* (1989, p. 612) that it began infilling within "a few months and years" and probably took a few decades to complete. Event R was thus interpreted to have occurred less than a decade or two before the lowermost sample (the lowermost 7 cm) of unit 59 peats (P59fl, Fig. 3). Using this description, we constrained the event R distribution using the local peat accumulation rate derived from the peat thick-

ness and the ordering constrained dates of P59fl and P59fu. This approach yields an estimate for event R of A.D. 1084 (1046–1113).

Both the longest and shortest recurrence intervals (discussed subsequently) and thus the estimated variability of earthquake recurrence at Pallet Creek depend on the date of event R. In addition, Sieh *et al.* (1989) regard event R as a candidate to have ruptured the entire southern San Andreas fault, so the likelihood of such a scenario depends critically on the date of event R. Events N and R are separated by a "major unconformity" (Sieh, 1984, p. 7658), and peats corresponding to unit 59 were not found anywhere in the extensive excavation area of Sieh (1984). If the fissure peats had not been found, or if somehow unit 59 peat formed before event R and was dropped or reworked into the fissure, the event would be dated by the constraints of Sieh (1984) as having occurred in the late 1100s or early 1200s. In this case both the longest and shortest recurrence intervals (R-T and N-R, respectively) would be much closer to the site average. The longest and shortest recurrence intervals largely control the estimated variability in large earthquake recurrence. This result highlights how a single stratigraphic inference can strongly affect subsequent conditional probabilities and recurrence predictions.

Event N: This event also occurred during a time when dating constraints are complex at Pallett Creek. Event N is separated from event R by at least the deposition of gravelly unit 53 and the cutting and filling of a 4.5-m-deep gully. Event N breaks upward through unit 52, which contains some peat and an incipient soil. We constrain the date distribution of event N by ordering and the peat thickness above P51 and below P53, leading to our mean estimate of A.D. 1067 (1031–1096). If we had included additional time for soil formation before event N, as did Sieh *et al.* (1989), its age would be closer to event R.

Event I: Peats P45u and P47, which bound event I, are in physical contact except where separated by sand blows. Sieh *et al.* (1989) cited this stratigraphic relationship as grounds to eliminate the older date range in P45u and to merge their sample ^{14}C ages to derive a narrowly confined estimate of A.D. 997 ± 13. The ^{14}C ages of P45u and P47 (1076.1 ± 17.1 and 1032 ± 11.3 B.P., respectively) do not strongly overlap, however, and their separation in radiocarbon age is consistent with their stratigraphic separation by approximately 2 cm of peat (Sieh *et al.* 1989, their table 2). We bounded event I by P45u and P47 and did not directly identify it with either. Our resulting event date distribution (914–986) overlaps with published values, but the mean, A.D. 956, is approximately 40 years older than that of Sieh *et al.* (1989).

Event F: this event occurred when unit 38 was the marsh surface. Sieh *et al.* (1989) combined the ^{14}C ages from P38u, P41, and P43 into a single ^{14}C age (1221 ± 9.2 years B.P.) and ascribed event F to the consequent calibrated date distribution, A.D. 797 (775–819). One centimeter of peat separates the centers of samples for layers P38u and P41 and about 4 cm of peat separates P38u and P43. At the local peat accumulation rate of 0.075 cm/yr, this amounts to 13 and 53 years, respectively. Considering the stratigraphic and radiocarbon evidence, we left layers P38u, P41, and P43 chronologically distinct and estimate event F to have occurred in about A.D. 842 (803–868).

Event D: Event D is well constrained by ordering alone and better constrained with peat accumulation constraints to about A.D. 764 (749–775). The quality of constraint reflects the large number of stratigraphically ordered samples in this portion of the section (Fig. 3) and their high degree of age overlap. The published estimate for event D (A.D. 734 ± 13) did not come from samples at the event horizon, but like event N, relied on the estimated dates of the events above and below it and on arguments based on the accumulation rate of fine-grained sediments. Sieh *et al.* (1989) also bounded event D using layer P33u, which lies several centimeters below the event horizon. The Bayesian approach permits event D to be dated directly from the constrained layer date distributions.

Event C: Our best estimate of event C is A.D. 645 (614–666). In this case, ordering constraint among the layers is sufficient to achieve most of this result, and event stratigraphic constraints add little.

Two older events at Pallett Creek, events A and B, are not included because the stratigraphic records of these events is fragmentary (Sieh, 1984; Sieh *et al.*, 1989).

Recurrence Intervals

Distributions for the time intervals $p_T(t)$ between events at a site can be computed from their respective empirical event pdfs (Fig. 6). Every pair of possible event dates $\{x_i, x_{i+1}\}$ from within p_{E_i} and $p_{E_{i+1}}$, respectively, is separated by some time $t = x_{i+1} - x_i$. In general many pairs $\{x_i, x_{i+1}\}$ can be separated by the same interval t. Recurrence interval pdfs are found by substituting $x_{i+1} = x_i + t$ in $p_{E_{i+1}}$ and repeating the sum for all values of t allowed by the range of $\{x_i, x_{i+1}\}$:

$$p_{T_i}(t) = \frac{\sum_{x=\min x_i}^{\max x_i} p_{E_{i+1}}(t + x) p_{E_i}(x)}{\sum_{\tau} \sum_{x=\min x_i}^{\max x_i} p_{E_{i+1}}(\tau + x) p_{E_i}(x)}, \qquad (4)$$

where $(0 < \tau < x_{i+1\,\max} - x_{i\,\min})$. Because equation (4) allows only positive separations between successive ruptures, the mean interval between events can be longer than the difference between the event means. This property of equation (4) only materially affects intervals N-R and W12-W11. Mean estimates of intervals between ruptures are shown in Figure 7 and summarized in Table 5. Intervals longer than the present open interval since 1857 are a minority at both sites, but are by no means exceptional.

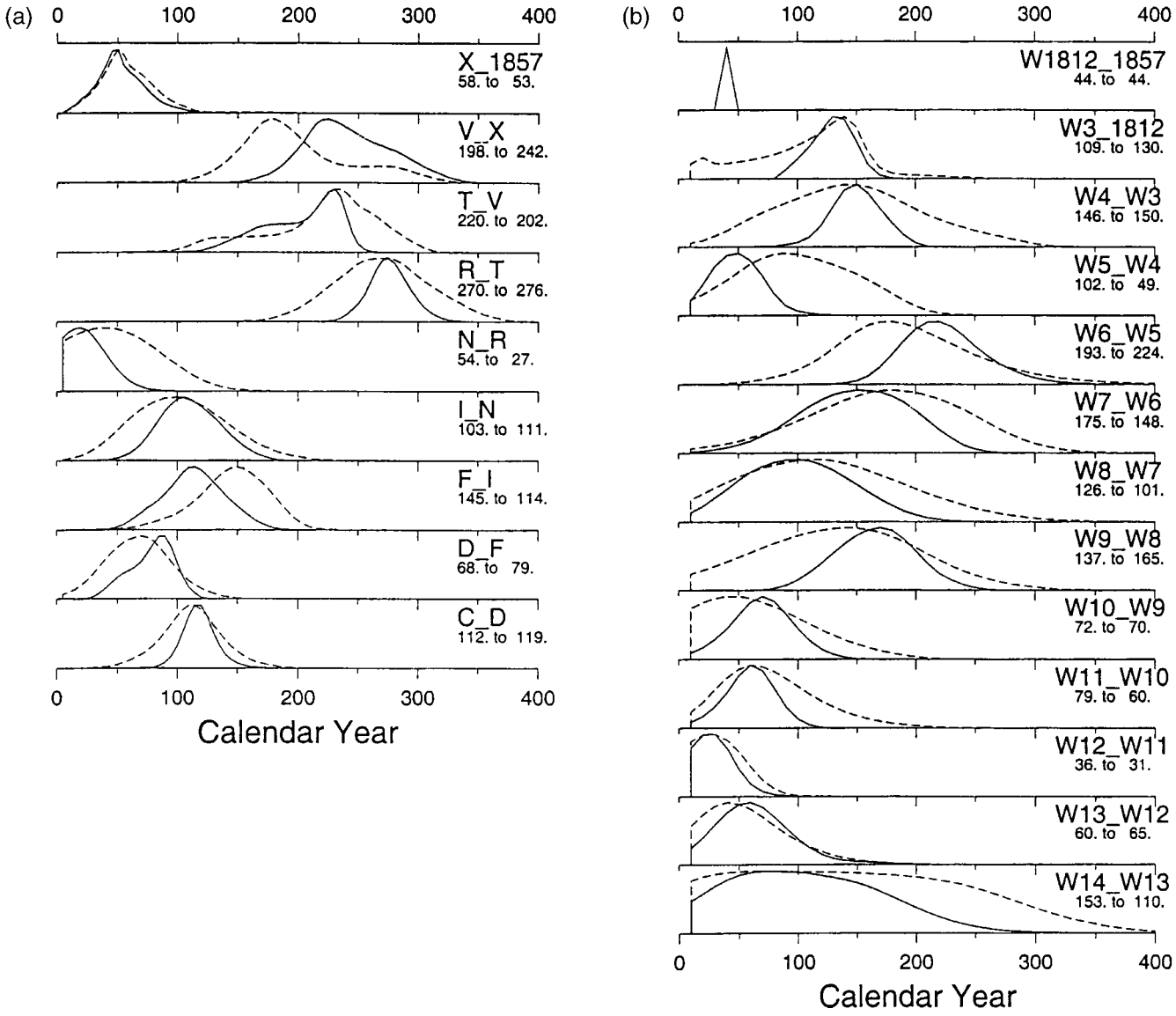

Figure 7. Recurrence intervals for (a) Pallett Creek and (b) Wrightwood. Mean recurrence intervals are shown for the best estimate (solid lines) and order-constrained (dashed lines) event dates from Figure 6.

Recurrence Model Parameter Estimation and Testing

Event pdfs from the previous section can be used directly in the estimation of conditional probabilities of a future event. Estimates of earthquake recurrence probability depend on the recurrence model used and on the uncertainty in the recurrence model parameters. We consider here Poisson, lognormal, and empirical distributions because each has been proposed to characterize large earthquake recurrence (e.g., Nishenko and Buland, 1987; Savage, 1994, WGCEP, 1995). Event dating uncertainty is included in conditional probabilities by drawing many event series at random from within the event pdfs and using conventional statistical tools on those series. Sample sizes were chosen qualitatively, based on consistency among repeated runs (Savage, 1991).

In proceeding with statistical modeling, the approximate nature of the correspondence between significant earthquakes and ground rupture events is recognized. For several reasons, however, we believe that this approximation is reasonable. First, the secular slip rate requires that over 3 m of slip per century, on average, be released in the area of the sites studied. Second, the slip-per-event and geologic evidences (Fumal *et al.*, 2002; Weldon *et al.*, 2002) are consistent with ground rupture by large earthquakes and would be difficult to explain by other mechanisms such as creep or a flurry of smaller events. Third, the two events for which something is known about ground shaking, in 1812 and 1857, both produced significant ground shaking at large distances from the fault. Thus, although individual earthquake magnitudes are not known, average and measured slip-per-

Table 5
Mean and 95% Range of Recurrence Distributions with Layer and Event Sediment Constraint*

	Full Constraint (.025–.975)		Ordering Only (.025–975)	
Events	Mean	Range	Mean	Range
Pallett Creek				
C:D	119	(90–146)	112	(58–163)
D:F	79	(37–108)	68	(15–121)
F:I	114	(60–162)	145	(78–195)
I:N	111	(61–160)	103	(30–182)
N:R	27	(10†–63)	54	(10†–122)
R:T	276	(240–311)	270	(193–346)
T:V	202	(134–243)	220	(115–290)
V:X	242	(176–314)	198	(121–299)
X:1857	53	(15–94)	58	(16–106)
Wrightwood				
W14:W13	110	(10†–231)	153	(10†–329)
W13:W12	65	(10†–140)	60	(10†–143)
W12:W11	31	(10†–63)	36	(10†–75)
W11:W10	60	(12–96)	79	(10†–172)
W10:W9	70	(13–118)	72	(10†–168)
W9:W8	165	(94–226)	137	(15–261)
W8:W7	101	(16–186)	126	(12–264)
W7:W6	148	(49–226)	175	(39–290)
W6:W5	224	(159–294)	193	(83–319)
W5:W4	49	(10†–89)	102	(12–191)
W4:W3	150	(98–188)	146	(31–266)
W3:1812	130	(88–158)	109	(10†–189)
W1812:1857	44			

*Distributions are plotted in Figure 8.
†Ten-year minimum estimate from geologic considerations.

event evidence suggest that statistical evaluation of the present event series can be meaningfully performed.

Poisson

The Poisson distribution uses a single parameter μ to characterize the probability of infrequent events that occur randomly in time. The probability of k events being observed in s units of time is

$$\Pr(Y = k;\ \mu,\ s) = P_y(k) = \frac{(\mu s)^k}{k!}\, e^{-\mu s}, \qquad (5)$$

where $1/\mu$ is the average recurrence time in years (Larson, 1982). Estimates of μ and 95% confidence ranges for Pallett Creek and Wrightwood are given in Table 6. Only dating uncertainty in the oldest event has any effect on the Poisson recurrence estimates because μ depends only on the total time interval and the number of events.

The Wrightwood and Pallett Creek average recurrence times (and ranges) are 105 (62–192) and 135 (74–282) years, respectively. The Poisson model probabilities of one or more earthquakes in the next 30 years for Pallett Creek and Wrightwood (Table 7) are 20% and 25% respectively, with respective ranges of 10%–33% and 14%–38%. These estimates depend little on the open interval since 1857.

We examine whether the paleoseismic event series are too strongly clustered or strongly periodic to have come from a Poisson parent distribution with two nonparametric tests of the Kolmogorov–Smirnov type. Both use a test statistic D, which is the greatest difference between the cumulative probability of a known distribution $\hat{F}(t)$ and an ordered sample $S(t)$ presumably derived from it. The test statistic D is calculated by

$$D = \max[|\hat{F}(t_j) - S(t_j)|],\ j = 1, \ldots, n_r, \qquad (6)$$

where n_r is the number of intervals in the sequence ($n_r = 9$ for Pallett Creek, and $n_r = 13$ for Wrightwood). Both tests use the property of a Poisson process that the time between successive events is an independent random sample from an exponential distribution.

The first test asks whether a change in the recurrence rate $1/\mu$ can be detected. This could occur if the recurrence intervals were strongly clustered. This test exploits the property of a Poisson process that, given first and last event times t_1 and t_{nr}, respectively, the intervening n_{r-1} event times are an independent random sample from a distribution uniform on (t_1, t_{nr}) (Diggle, 1990, p. 100). The actual event times $t_2, \ldots, t_{nr-1}$ are used in $S(t_j) = (t_j - t_1)/(t_{nr} - t_1)$, $j = 2, \ldots, n_{r-1}$, to form a time-ordered sample that may be compared to a cumulative uniform distribution $\hat{F}(t) = t$ on (0,1). Results (Fig. 8) indicate that neither the Pallett Creek nor Wrightwood event series is strikingly more clustered than might be expected from its corresponding Poisson process.

The second test uses equation (6) to examine whether an observed series is too regular to have derived from a Poisson process. In this test, recurrence intervals are ordered by length as $T(1), T(2), \ldots, T(n_r)$ and compared with a random sample drawn from the exponential distribution. We compare $S(t)$, the fraction of observed intervals T less than or equal to t ($0 < t < \infty$) to $\hat{F}(t) = [1 - \exp(\hat{\mu}t)]$. Because the Poisson parameter $\hat{\mu}$ must be estimated from the sample, the critical value against which to test D must be chosen accordingly (Mason and Bell, 1986). A series showing regularity of recurrence will appear as a nearly vertical sequence of steps in the cumulative plot $S(t)$. The tests of regularity for Pallett Creek and Wrightwood are shown in Figure 9. The Wrightwood series is somewhat more regular than would be predicted from a Poisson recurrence model, but neither series is sufficiently anomalous to exclude the Poisson model.

Lognormal

The lognormal distribution of recurrence intervals has been advocated by Nishenko and Buland (1987) and has been used by the Working Group on California Earthquake Probabilities (WGCEP) (1988, 1990, 1995) to estimate the conditional probabilities of earthquakes on the San Andreas fault. The lognormal distribution,

$$p(T,\ \overline{T},\ \sigma_{ln}) = \frac{1}{(2\pi\overline{T})^{1/2}} \exp\left[\frac{-\ln(T/\overline{T})^2}{2\sigma_{ln}^2}\right], \qquad (7)$$

Table 6
Most Likely Parameters and 95% Ranges for Poisson and Lognormal Model Parameter Estimates

	Poisson				Lognormal	
Site	Events	Interval	Average (Years)	μ (Range)	$\hat{\bar{T}}$	$\hat{\sigma}_{\ln}$
Pallett Creek	10	645 to 2001	135 (74–282)	.0074 (.0135–.0035)	107 (65–178)	0.76 (0.51–1.45)
Wrightwood	14	534 to 2001	105 (62–192)	.0095 (.0160–.0052)	83 (57–123)	0.70 (.50–1.15)

Table 7
Thirty-Year Conditional Probability Estimates of a Future Event for the Poisson, Lognormal, and Empirical Distributions

Site	Poisson	Lognormal	Empirical
Pallett Creek	20% (10%–33%)	25% (7%–42%)	29% (5%–62%)
Wrightwood	25% (14%–38%)	34% (17%–49%)	46% (17%–76%)

models the natural log of recurrence intervals $T_{\mathbf{i}}$ as normally distributed about a median $\overline{T}$ with variance $\sigma^2_{\ln}$ (Savage, 1991). $\overline{T}$ and its standard error σ_{T} were estimated for n_{r} intervals by $\ln \hat{\bar{T}} = n_{\mathrm{r}}^{-1}\, \Sigma \ln T_i$ and $\hat{\sigma}_T = \hat{\sigma}_{\ln}/n_{\mathrm{r}}^{1/2}$, respectively, and $\sigma^2_{\ln}$ was estimated by $\hat{\sigma}^2_{\ln} = \Sigma[\ln(T_i/\overline{T})]^2/(n_{\mathrm{r}} - 1)$.

Table 6 provides average lognormal parameter values and 95% confidence ranges for 1000 trials for the Wrightwood and Pallett Creek event distributions. This approach thus incorporates event dating uncertainty directly into parameter estimates $\hat{\bar{T}}$ and $\hat{\sigma}_{\ln}$. Monte Carlo picks of very short recurrence intervals such as between events N and R (Fig. 7b) greatly increase the width parameter $\hat{\sigma}_{\ln}$. Event dates are well enough resolved that dating uncertainty contributes only secondarily to the two-standard-error range of $\hat{\bar{T}}$ and $\hat{\sigma}_{\ln}$.

Lognormal variances $\hat{\sigma}_{\ln}$ are 0.70 and 0.76 for Wrightwood and Pallett Creek, respectively. Weak time predictability is implied by $\hat{\sigma}_{\ln} < 1$. Weak time predictability can arise as a numerical consequence of normalizing by the mean interval length for short earthquake series (Goes, 1996), but this effect should be minor for event series as long as the present ones. Distributions are shown in Figure 10 of 30-year conditional probabilities of a future earthquake given that the last major event occurred in 1857. To incorporate uncertainty in both $\hat{\bar{T}}$ (Savage, 1991) and the event dates themselves we first draw an event series from the event date distributions to get $\hat{\bar{T}}$. Each estimate $\hat{\bar{T}}$ itself has a lognormal distribution from which we select many values of $\overline{T}$ with which to estimate conditional probabilities. Thirty-year conditional probabilities are 25% (7%–42%) for Pallett Creek, 34% (17%–49%) for Wrightwood. The uncertainty in conditional probabilities is due to the wide formal range of possible $\hat{\bar{T}}$ and $\hat{\sigma}_{\ln}$ values, which can be reduced only as the square root of the number of intervals.

Empirical

Savage (1994) suggested that the conditional probability of a future event might be estimated from the observed recurrence intervals alone. We here extend his method to include dating uncertainties of paleoseismic series. If n observed intervals are considered to start at the date of the last event, some m of them would fall in any subsequent interval $(T, T + \Delta T)$. With success defined as an event falling in interval $(T, T + \Delta T)$, and failure otherwise, the distribution governing the probability P of a future event in $(T, T + \Delta T)$ is a beta distribution:

$$P(p|m,n) = \frac{(n+1)!}{m!(n-m)!}\, p^m (1-p)^{n-m}, \qquad (8)$$

with estimated mean $\hat{p} = (m + 1)(n + 1)$ and variance $\hat{\sigma}^2 = \hat{p}(1 - \hat{p})/(n - 3)$. Conditional probabilities $P(p|m', n', T > 145 = 2002 - 1857)$ of an event in the next 30 years are found by counting m', the number of intervals that from 1857 would predict an event in the next 30 years, and n', the number of intervals exceeding the present open interval. We again draw at random from the event distributions and form estimates $\hat{p}$ and $\hat{\sigma}^2$ from the resulting intervals. Results averaged over 100 trials are summarized in Table 7. Uncertainties p_{lo} and p_{hi}, representing 5% and 95% bounds for $\hat{p}$, are found from, respectively,

$$\int_{-\infty}^{p_{\mathrm{lo}}} P(p|m,n)dp = .05 \text{ and } \int_{-\infty}^{p_{\mathrm{hi}}} P(p|m,n)dp = .95. \qquad (9)$$

Because m' is often 0 during the next 30-year interval (2002–2032), $\hat{p}$ is only slightly greater than $1/(n' + 1)$ for all event records. For Pallett Creek and Wrightwood, $\hat{p} =$ 29% (5%–62%) and 46% (17%–76%), respectively. The large uncertainties in empirical distribution conditional probabilities show that even the present long paleoseismic series do not constrain uncertainties when relatively few interval lengths are longer than the open interval since 1857. In essence there is not much information in the empirical distribution with which to predict the fault's behavior from past intervals alone.

Discussion

Quantitative Analysis

As results for the Pallett Creek and Wrightwood sites indicate, the systematic use of available quantitative information provides a relatively objective starting point for event dating and subsequent interpretation. Systematic use of ordering relationships among layers may or may not also yield

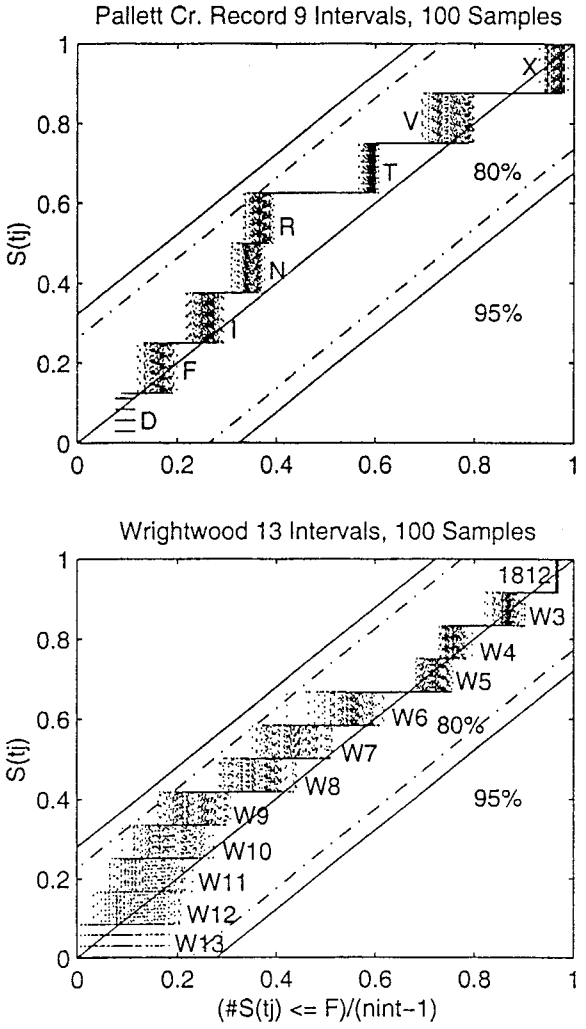

Figure 8. Nonparametric test for clustering at Pallett Creek and Wrightwood. Event series were chosen at random from the fully constrained pdfs of Figure 6. Horizontal increments are the fraction of the total time from event C or W14 to 1857 taken by each interval ending at the labeled event. One vertical step is taken at each event and plotted as a dotted line. Repeating the sampling 100 times results in apparent increases and decreases in line density, which reflect more or less commonly selected paths. Series that cross the 80% and 95% bounds are too clustered at that level of confidence to have derived from a Poisson distribution. The series culminating at event R would not be unusual (i.e., expected 20%–30% of the time) for a Poisson process. The long step from event R to event T illustrates the importance of the stratigraphic relations around event R to the hypothesis of clustering.

greater precision. The systematic approach may also highlight points where greater precision depends on subjective and potentially controversial interpretations. Even where the quantitative approach leads to unlikely results, it serves to highlight the interpretational and data issues needed to resolve them.

In regard to paleoseismic data collection and analysis, Figures 2 and 3 show that as one is deciding how to sample at a new site, ordered samples have the potential to yield greater resolution than the same number of samples focused on the event-bounding layers. Replicate sampling can be used to obtain increased precision in the ^{14}C age, but one might discover that the calendric range of the layer is still poorly resolved, or that one has precisely determined an inconsistent ^{14}C age. The former can occur because the precise ^{14}C age yields a multimodal calendric distribution or falls on a flat spot in the calibration curve. The latter could occur because of contamination or sample pretreatment (e.g., Seitz, 1999). Layer P72 constraining Pallett Creek event V illustrates both of these possibilities. Ages of samples of P72 appear to be too old for the stratigraphic position of this layer, but if it had a slightly younger ^{14}C age, it would fall on a wide, multivalued portion of the calibration curve. Ordered samples may be more likely to identify inconsistencies and yield event dates less dependent on individual dates. The methods presented here provide a potentially valuable improvement in paleoseismic dating accuracy in that they rely more on the consistent elements of all the data and less on any particular measurement. In this sense, they make the results more robust.

The quantitative analysis procedures applied here have some properties one must keep in mind when applying them. For example, it is assumed that layer dates bounding an event horizon constitute legitimate bounds to the event date. With bounding peat dates, this assumption is relatively secure, and, ideally, ordering relationships can test it. However, when the available carbon source did not accumulate in place, as might be the case if wood fragments or detrital charcoal occur in the peat, equation (3) should be used with caution. It is also assumed that it makes sense to say that the event is equally likely at any time within the bounds or bounds adjusted by sedimentation constraints (Fig. 5). When the upper date is separated by a depositional hiatus and an unknown amount of time has passed, it is technically true to the data, if somewhat unsatisfying, to say that the best estimate event date falls approximately halfway between the bounding layer dates. However, in some cases the midpoint is known to postdate the event. For example, subduction earthquakes in the Pacific Northwest are no doubt closer in time to the highest coseismically submerged freshwater flora than to the lowest salt marsh plants of the interseismic emergence phase (e.g., Atwater *et al.*, 1995). Such a case violates the "equally likely in the interval" assumption in Figure 5. One might attempt to compensate by changing the shape of the prior between bounding dates (equation 2), but the shape could be difficult to quantify. In cases where the event is usefully bounded only on one side, it may be preferable to pursue ordered samples below the event horizon where they can eliminate spurious modes in the calendric distribution of the topmost sample. In general, the greater the separation between the dating constraints, the more important consideration of the "equally likely" assumption in Figure 5 becomes.

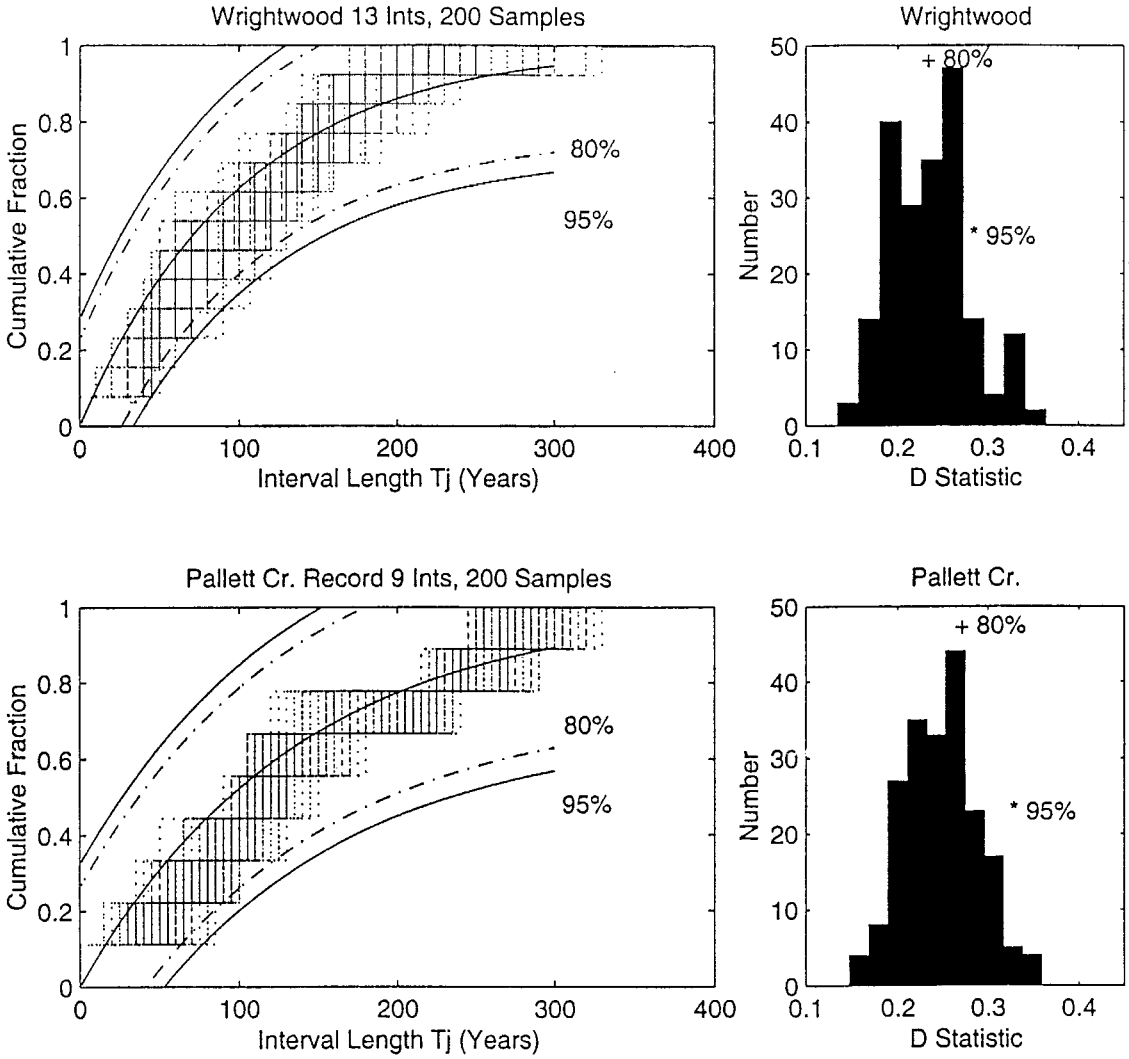

Figure 9. Nonparametric test comparing ordered samples from an exponential distribution of recurrence intervals, as would be generated by a Poisson process. Each sample series (100 total) is plotted with a dotted line so more frequently chosen series appear with greater line density. Series crossing 80% and 95% bounds are too regular at those levels of significance for a likely Poisson process. Histograms of the *D* statistic show that a Poisson recurrence distribution cannot be ruled out for either event series.

Recurrence Models and Conditional Probabilities

The sampling methods illustrated here show that uncertainties in dating relationships can be carried to recurrence model parameters and conditional probabilities without modifying individual event date uncertainties. Sampling can also incorporate uncertainty in recurrence model parameters by applying a two-tiered approach, sampling first from the event series and then from an uncertainty function associated with the parameter estimate. The Pallett Creek and Wrightwood series illustrate that the formal uncertainty in the mean and variance parameters due to the brevity of the event sequence is comparable to or greater than the uncertainty due to dating. This is most apparent for the Poisson model (Figs. 9, 10), where dating uncertainty is only relevant in the oldest event and thus has little capacity to affect the Poisson mean parameter. When the observed event sequence is inverted for the likely range of Poisson parameters that could have given rise to it, uncertainty blossoms to the wide ranges shown in Table 6. Longer records help reduce the formal uncertainties, but they do so slowly, by the square root of the number of recurrence intervals. Considering the difficulty of obtaining a record of even a few events, parametric uncertainty is likely to present a practical limitation on single-site conditional probability estimates from paleoseismic records.

Both the Pallett Creek and Wrightwood sequences have runs of shorter than average recurrence intervals (e.g., W13–W10, W8–W6, C–D–F, and I–N–R) that ended with longer or much longer than average intervals. This appearance led

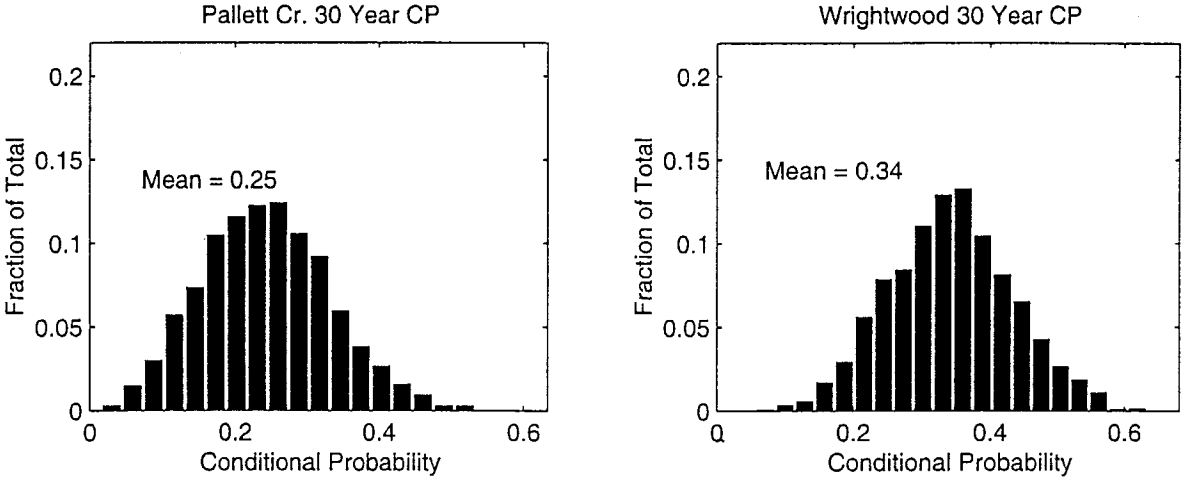

Figure 10. Lognormal conditional probability (CP) plots for future events at Wrightwood and Pallett Creek. We used a two-level Monte Carlo technique. To account for dating error, events are drawn at random from the appropriate series (Fig. 6). The $\hat{T}$ estimate for each event set is then deviated at random by up to two standard errors to account for parametric uncertainty. The conditional probability is calculated for each case and compiled for the histogram display. Variability among runs amounted to $\pm 0.5\%$ in the conditional probability estimates.

Sieh *et al.* (1989) to suggest that the Pallett Creek series is clustered. In the sense of their usage, Wrightwood might be considered clustered as well. However, neither the Wrightwood nor Pallett Creek event chronologies are more clustered than would be likely from a Poisson distribution. This conflict of appearances and statistics highlights a relevant issue. While it is straightforward to estimate parameters for a recurrence model from an event series, it is difficult to validate that model because of the natural scatter in the data and the relative weakness of tests to disprove it. In a clustering model, one may solve for, say, average long and average short interval lengths and a rule for deciding how to pick one or the other. Three or more parameters must be estimated from the event series. This leaves too few degrees of freedom to then demonstrate the legitimacy of the model. Thus, while some patterns including clustering might be suggested by eye, their significance cannot be proven with the data at hand.

Recurrence Patterns and Fault Behavior

Though we cannot prove that the present earthquake series (Fig. 6) do not come from a random process, both site records suggest a relative acceleration of activity from the early 600s to the early 800s, followed by a lower rate through around A.D. 1500, and followed again by a higher rate. The details differ among sites (and depend on the event R-P59 relationship, among other things), but both indicate that some form of short-term variation in rate may be occurring. The reasons for this variation are at present speculative. Many earthquake recurrence models have a memory in the sense that the size or interval between events depends on the size of the previous quake or interval, or predicts the future interval or earthquake size. These are often called time or slip predictable models (e.g., Scholz, 1990; McCalpin, 1996). Given that ground rupturing earthquakes on the southern San Andreas fault appear to have similar displacements on the fault, we do not consider variations in displacement as a likely mechanism to provide feedback between earthquakes. Alternative explanations fall into three categories: (1) variations in the strain accumulation rate; (2) interactions between faults or parts (segments) of the same fault; and (3) variations in the physical state of the fault.

Variations in the secular strain accumulation rate could easily explain periods of long or short recurrence intervals if such changes could be justified from geodetic or geologic observation. However, we are unaware of any observations that suggests that the processes driving the motion of crustal blocks vary on timescales of hundreds to thousands of years. We consider variation in far-field loading rate to be unlikely and, in any event, untestable until elastic strain accumulation can be measured over several earthquake cycles.

On the other hand, fault interaction, or strain transfer, due to earthquakes on other segments of the same fault or different faults, does appear to affect the timing of earthquakes (e.g., Izmit and Duzce, Turkey, 1999; Landers and Hector Mine, California, 1992 and 1994, respectively). Because the San Andreas fault is essentially two-dimensional, it is hard to imagine how segment interactions could cause a cluster of four or five events like those observed in the Wrightwood record. Perhaps a more likely possibility is modulation by a nearby fault that has a recurrence interval on the order of the longer-term variability our data seem to suggest. Palmer *et al.* (1995) show that recurrence intervals can be modulated by accumulation and release of fault-normal stresses at restraining bends in the fault. Restraining and releasing bend structures have been mapped along this

section of the fault (Weldon and Springer, 1988), including the Cleghorn fault near Wrightwood and the Punchbowl fault near Pallett Creek. Alternatively, the fault-normal stresses might be modulated by more distant fault interaction, such as with the thrust system on the south side of the San Gabriel Mountains or perhaps the northern frontal fault of the San Bernardino Mountains.

In the category of variations in fault physical state, we include strain conditioning of the recurrence interval. Earthquake recurrence may be relatively regular for a while, but incompletely release stress, causing strain to accumulate. In time, however, recurrence is restored to a mean behavior with a probability that increases with the distance that the fault is from some mean strain state. Alternatively, one could hypothesize that physical properties of the fault zone could vary through time. For example, the characteristic size or spacing of asperities might influence how easily rupture initiates, and also how the strength of the fault evolves with time. Although the event series we discuss here are too short to confidently establish longer-term fault behavior, it is important to recognize that models of the fault have consequences for recurrence behavior and that an earthquake series long enough to test these physical and statistical models remains an important goal for paleoseismology.

Event Correlations

Event correlations between paleoseismic sites are usually difficult to demonstrate with ^{14}C dating alone. Even when the event distributions strongly overlap, dating alone cannot resolve whether one event disturbed both sites, or whether there were simply two events close together in time. However, where meters of slip are observed, faults tend to rupture for tens to hundreds of kilometers (Hemphill-Haley and Weldon, 1999), so correlation between Pallett Creek and Wrightwood events must be considered.

1857: This correlation is historically based (Sieh, 1978b) and is consistent with stratigraphic and radiocarbon evidence. X-1812: As concluded by Sieh *et al.* (1989), dendrochronological evidence of a ground-rupturing earthquake between the Wrightwood and Pallett Creek sites in the winter of 1812–1813 (Jacoby *et al.*, 1988), and historical evidence for a large southern California earthquake at this time make this correlation almost certain. Ordering constraints reinforce this case by eliminating nearly all of the range of event X before the start of the historical record, including a range of event X in the late 1600s originally allowed by Sieh *et al.* (1989). X-W3: Fumal *et al.* (1993) suggested this correlation based on the small range of X in the late 1600s allowed by Sieh *et al.* (1989). Fumal *et al.* (1993) argued that because the deformation associated with event W3 is greater than for W1812, it is more likely to have extended to Pallett Creek and correlate with the large offset associated with event X (Sieh, 1984). Their hypothesis, which limits the northwestern extent of the 1812 rupture to between Wrightwood and Pallett Creek, also seemed to them more consistent with the ground-shaking intensity records. However, the ordering constrained range of event X presented here virtually excludes the correlation of events W3 and X. Event W3 appears to have occurred during the interval between Pallet Creek events V and X. V-W4: The fully constrained distributions of events V and W4 overlap by about 38%, measured by their areas of intersection. If these represent the same event, it occurred within a couple of decades of A.D. 1536, the mean estimate for event W4. This estimate is similar to what would be inferred if event V is considered to shortly postdate layer P68, as originally held by Sieh (1984). V-W5: The fully constrained distributions for events W5 and V overlap by less than 1%, so it appears that W5 is a separate event that occurred between events T and V at Pallett Creek. If samples from the five layers below event V are incorrect (Fig. 3), despite their internal consistency, and the date of layer P72 is correct, then event V would correlate reasonably well with event W5. R-W6: The correlation of events R and W6 depends on whether R predates or postdates unit 59 peat. If, as reported, the peat in the fissure accumulated after event R, it would not correlate with event W6. If R actually postdates P59u peat, the younger range of R would overlap sufficiently with the older range of W6 that these events might correlate. R-W7 or N-W7: The younger range of R, if it predates the P59 peats, overlaps with the older range of W7, so this and the alternative association of N with W7 around A.D. 1070 depend critically on the event R-P59 peat relationship. I-W8: The constrained distributions of I and W8 overlap sufficiently to suggest a correlation, though not with much likelihood, around A.D. 980. Events I, N, and R and W6, W7, and W8 form triplets separated by relatively long intervals at each site. Thus it is tempting to suggest that they correlate despite their limited overlap in ages. Events I, N, and R are systematically older than W8, W7, and W6, respectively, in their suggested pairings, suggesting systematic contamination of old carbon in layers containing events I, N, and R, or of young carbon in layers bounding events W6, W7, and W8. F, D, and C-W9, W10, W11, W12, and W13: Five Wrightwood events occur during the same interval over which only three events were observed at Pallett Creek. Constrained distributions for events F and W9 overlap almost identically near A.D. 850, while events C and W13 coincide within a few years around A.D. 640. Event D coincides best with event W10 near A.D. 770 using the present analysis, but would match event W11 somewhat better if the Sieh *et al.* (1989) estimate in the 730s is sustained. Realistically, the dating resolution allows other pairings as well, but the mismatch in the number of events and their relative concentration in time at both sites during this period is clear.

Events that do not correlate between the two sites may have ruptured a portion of the fault not including the other site or, in principle, may have been missed during periods of low sedimentation rates or periods when only massive units were accumulating. Sieh *et al.* (1989) considered the interval between events R and T as a possible place for a missing event at Pallett Creek because of the massiveness of

unit 59 sediments postdating event R, but they did not consider any missing events likely. Event W3 occurred during a period of low sedimentation at Pallett Creek between events V and X. Sieh *et al.* (1989) considered the record in this portion of their section to be complete, but K. Sieh (personal comm., 1993) indicated that there is some evidence for a disturbance at the site at about this time. Event T occurred during the longest interevent interval in the present Wrightwood record. The lack of resolvable stratigraphy in the thick W130 peat layer makes identification of events during this time difficult, and a missing event during accumulation of this peat is considered possible. Whether any events have been missed at either site, the existence of 13 or possibly 14 events at Wrightwood during the same interval that 10 events occurred at Pallett Creek suggests interactions and potentially complex rupture behavior along this reach of the San Andreas fault.

Conditional Probabilities of Earthquake Recurrence

Mean estimates of conditional probabilities of earthquake recurrence in the next 30 years are somewhat higher at Wrightwood than at Pallett Creek, reflecting the greater number of events in a similar overall amount of time. Uncertainties in conditional probabilities are somewhat reduced by the longer event series at Wrightwood for the same reason. The Poisson model suggests approximately 20% and 25% probabilities of a ground-rupturing event in 30 years for Pallett Creek and Wrightwood, respectively. Mean lognormal probabilities are 25% and 34%, respectively. These estimates are in line with estimates by the WGCEP (1995). The greater probability estimates under the lognormal model reflect the presence of a degree of time predictability in the records studied. The high degree of correspondence between the two records and indications that events at each site may occur during the longest interseismic intervals of the other offer further, tantalizing clues of some greater underlying predictability.

Acknowledgments

This research was supported by U.S. Geological Survey Grants 1434-93-G-2286 and 1434-HQ-97-GR-03117, NSF EAR 9057014, NSF EAR 8920136 and PG&E 024199#1 through the Southern California Earthquake Center to R. Weldon and National Earthquake Hazard Reduction Program (NEHRP) grant 1434-95-G2532. Additional support for G.P.B. was provided from NSF EAR 9018435 to E. Humphreys. Work was also performed under contract W-7405-Eng-48 by U.S. Department of Energy to the University of California Lawrence Livermore National Laboratory. We thank K. Sieh for sharing data and clarifying points of stratigraphy, J. Savage for his statistical insights, and D. Jackson for early correspondence leading to much-improved statistical testing and later as a reviewer. We also thank Doug Yule for his thorough and thoughtful review.

References

Atwater, B. F., A. R. Nelson, J. J. Clague, G. A. Carver, D. K. Yamaguchi, P. T. Bobrowsky, J. Bourgeois, M. E. Darienzo, W. C. Grant, E. Hemphill-Haley, H. M. Kelsey, G. C. Jacoby, S. P. Nishenko, S. P. Palmer, C. D. Peterson, and M. A. Reinhart (1995). Summary of coastal geologic evidence for past great earthquakes at the Cascadia subduction zone, *Earthquake Spectra* **11,** 1–18.

Biasi, G., and R. J. Weldon II (1994). Quantitative refinement of calibrated C-14 distributions, *Quaternary Research* **41,** 1–18.

Diggle, P. J. (1990). *Time Series*, Oxford University Press, Oxford, U.K., 257 pp.

Fumal, T. E., S. K. Pezzopane, R. J. Weldon II, and D. P. Schwartz (1993). A 100-year average recurrence interval for the San Andreas fault at Wrightwood, California, *Science* **259,** 199–203.

Fumal, T. E., R. J. Weldon II, G. P. Biasi, T. Dawson, G. G. Seitz, W. T. Frost, and D. P. Schwartz (2002). Evidence for large earthquakes on the San Andreas fault at the Wrightwood, California, paleoseismic site: A.D. 500 to present, *Bull. Seism. Soc. Am.* **92,** no. 7, 2726–2760.

Goes, S. D. B. (1996). Irregular recurrence of large earthquakes: an analysis of historic and paleoseismic catalogs, *J. Geophys. Res.* **101,** 5739–5749.

Hemphill-Haley, M. A., and R. J. Weldon II (1999). Estimating prehistoric earthquake magnitude from point measurements of surface rupture, *Bull. Seism. Soc. Am.* **89,** 1264–1279.

Jacoby, G. C., P. R. Sheppard, and K. E. Sieh (1988). Irregular recurrence of large earthquakes along the San Andreas fault: evidence from trees, *Science* **241,** 196–199.

Larson, H. J. (1982). *Introduction to Probability Theory and Statistical Inference*, John Wiley and Sons, New York, 637 pp.

Mason, A. L., and C. B. Bell (1986). New Lilliefors and Srinivasan tables with applications, *Commun. Stat. Sim. Comp.* **15,** 451–477.

McCalpin, J. P. (1996). *Paleoseismology*, Academic Press, New York, 588 pp.

Nishenko, S. P., and R. Buland (1987). A generic recurrence interval distribution for earthquake forecasting, *Bull. Seism. Soc. Am.* **77,** 1382–1399.

Palmer, R., R. Weldon, E. Humphreys, and F. Saucier (1995). Earthquake recurrence on the southern San Andreas modulated by fault-normal stress, *Geophys. Res. Lett.* **22,** 535–538.

Salyards, S. L., K. E. Sieh, and J. L. Kirschvink (1992). Paleomagnetic measurement of non-brittle coseismic deformation across the San Andreas fault at Pallett Creek, *J. Geophys. Res.* **97,** 12,457–12,470.

Savage, J. C. (1991). Criticism of some forecasts of the National Earthquake Prediction Evaluation Council, *Bull. Seism. Soc. Am.* **81,** 862–881.

Savage, J. C. (1994). Empirical probability distributions from observed recurrence intervals, *Bull. Seism. Soc. Am.* **84,** 219–221.

Scholz, C. H. (1990). The *Mechanics of Earthquakes and Faulting*, Cambridge University Press, New York, 439 pp.

Seitz, G. G. (1999). The paleoseismology of the southern San Andreas fault at Pitman Canyon: implications for fault behavior and paleoseismic methodology, *Doctoral Dissertation*, University of Oregon, Eugene, 278 pp.

Sieh, K. (1978a). Prehistoric large earthquakes produced by slip on the San Andreas fault at Pallett Creek, California, *J. Geophys. Res.* **83,** 3707–3939.

Sieh, K. (1978b). Slip along the San Andreas fault associated with the great 1857 earthquake, *Bull. Seism. Soc. Am.* **68,** 1421–1428.

Sieh, K. E. (1984). Lateral offsets and revised dates of large earthquakes at Pallett Creek, California, *J. Geophys. Res.* **89,** 7641–7670.

Sieh, K., M. Stuiver, and D. Brillinger (1989). A more precise chronology of earthquakes produced by the San Andreas fault in southern California, *J. Geophys. Res.* **94,** 603–623.

Stuiver, M., and P. Reimer (1993). Extended ^{14}C data base and revised CALIB 3.0 ^{14}C age calibration program, *Radiocarbon* **35,** 215–230.

Toppozada, T. R., C. R. Real, and D. L. Parke (1981). Preparation of isoseismal maps and summaries of reported effects for pre-1900 California earthquakes, *Calif. Div. Mines Geology Open-File Rept. 81-11*.

Ward, G. K., and S. R. Wilson (1978). Procedures for comparing and combining radiocarbon age determinations: a critique, *Archaeometry* **20,** 19–31.

Weldon, R. J., II, and Springer, J. E. (1988) Active faulting near the Cajon Pass well, southern California: implications for stress orientation near the San Andreas fault, *Geophys. Res. Lett.* **15,** 993–996.

Weldon, R. J., II, T. E. Fumal, T. P. Powers, S. K. Pezzopane, and J. C. Hamilton (2002). Structure and earthquake offsets on the San Andreas fault at the Wrightwood, California, paleoseismic site, *Bull. Seism. Soc. Am.* **92,** no. 7, 2704–2725.

Working Group on California Earthquake Probabilities (WGCEP) (1988). Probabilities of large earthquakes occurring in California on the San Andreas fault, *U.S. Geol. Sur. Open-File Rep. 88-398*.

Working Group on California Earthquake Probabilities (WGCEP) (1990). Probabilities of large earthquakes occurring in San Francisco Bay region, California, *U.S. Geological Survey Circular 1053*.

Working Group on California Earthquake Probabilities (WGCEP) (1995). Seismic hazards in southern California: Probable earthquakes, 1994 to 2024, *Bull. Seism. Soc. Am.* **85,** 379–439.

Appendix

Table A1
Table Associating Radiocarbon Dates with Layers and Layer Peat Thicknesses

Layer	Lab Identifier	C14 Age	Std Dev	Lab Multiplier	Peat Thickness (cm)
W135g	QL_4396	116	22.5	1.6	5
W135g	US_2731	140	55	1	
W135f	CAMS_72555	260	30	1	4
W135f	CAMS_72554	300	40	1	
W135e	QL_4398	137	22.5	1.6	4
W135e	US_2788	215	65	1	
W135d	US_2789	280	65	1	3
W135d	US_2737	285	40	1	
W135d	QL_4399	302	22.5	1.6	
W135b	QL_4397	334	21	1.6	3
W135b	US_2798	385	55	1	
W135a	US_2790	385	65	1	3
W130u	CAMS_72559	500	40	1	3
W130u	CAMS_72560	510	40	1	
W130u	US_2733	440	60	1	
W130u	US_3121	440	50	1	
W130	B-25588	420	70	1	7
W130	US_2631	565	45	1	
W130	US_2632	590	45	1	
W130	B-23346	590	60	1	
W130L	B-114065	590	60	1	7
W130L	QL_4945	597	14	1.6	
W130L	US_3132	625	40	1	
W125c	CAMS_72548	800	40	1	1
W125c	CAMS_72549	810	40	1	
W125c	CAMS_73690	850	60	1	
W125c	US_2635	850	45	1	
W125c	US_2634	865	50	1	
W125c	B-25596	890	60	1	
W125c	QL-4946	890	20	1.6	
W125b	US_2796	840	50	1	2
W125b	QL-4947	956	15	1.6	
W125b	QL-4938	960	20	1.6	
W125a	QL-4939	975	21	1.6	4
W125a	QL-4948	1019	12	1.6	
W125a	US 2627	985	50	1	
W122	B-25587	990	70	1	2
W120c	QL-4940	971	20	1.6	3
W120c	US_2633	1085	40	1	
W120c	B-25592	1130	70	1	
W120b	US_2795	1025	50	1	2
W120b	QL-4941	1215	21	1.6	
W120a	US_2736	1100	40	1	2
W120a	B-25593	1250	60	1	
W120a	QL-4942	1176	21	1.6	
W115	US_2638	1205	40	1	6
W115	US_2637	1215	40	1	
W115	CAMS_72543	1070	40	1	
W115	CAMS_72542	1030	40	1	
W115	CAMS_72544	1150	40	1	
W115	B_114072	1040	60	1	
W115	QL-4943	1212	15	1.6	
W115	QL-4944	1222	15	1.6	
W110d	CAMS_72553	1210	40	1	4
W110d	CAMS_72552	1180	40	1	
W110d	US_2734	1230	40	1	
W110c	US_2797	1305	40	1	1
W110b	US_2791	1305	40	1	1
W110a	US_2792	1295	35	1	1
W105d	CAMS_72557	1260	40	1	1
W105d	CAMS_72556	1320	30	1	
W105d	CAMS_72558	1270	40	1	
W105	US_2628	1275	45	1	1
W105	US_2629	1295	40	1	
W105	B-25590	1270	70	1	
W100c	CAMS_73691	1140	50	1	2
W100c	CAMS_72547	1360	30	1	
W100c	US_2735	1450	45	1	
W100b	US_2794	1730	60	1	4
W100a	US_2793	1750	40	1	4
W97	B26354	1770	60	1	0.5

Seismological Laboratory, MS-174
University of Nevada–Reno
Reno, Nevada 89557
(G.P.B.)

Department of Geological Sciences
University of Oregon
Eugene, Oregon 97403-1272
(R.J.W.)

U.S. Geological Survey
Earthquake Hazards Team, MS 977
345 Middlefield Rd
Menlo Park, California 94025
(T.E.F.)

Lawrence Livermore National Laboratory
Center for Accelerator Mass Spectrometry
7000 East Avenue, L397
Livermore, California 94551
(G.G.S.)

Manuscript received 22 May 2001.